https://doi.org/10.15407/ufm.27.02.304

V.B. TARELNYK [1,*], O.P. HAPONOVA [2,3,], N.V. TARELNYK [1,***], Ie.V. KONOPLIANCHENKO [1,****], M. A. MIKULINA [1], and V.V. POSTOLATII [1]**

[1] Sumy National Agrarian University,
160 Herasyma Kondratieva St., UA-40021 Sumy, Ukraine
[2] Sumy State University, 116 Kharkivska St., UA-40007 Sumy, Ukraine
[3] Institute of Fundamental Technological Research,
Polish Academy of Sciences, 5B Pawińskiego, 02-016 Wársaw, Poland

* tarelnyk@ukr.net, ** gaponova@pmtkm.sumdu.edu.ua,
*** natashatarelnik@ukr.net, **** konoplyanchenko@ukr.net

IMPROVING THE QUALITY PARAMETERS OF STEEL SURFACES BY COMBINED ELECTROSPARK CARBURIZING TECHNOLOGIES. Pt. 1. Properties of Metal Surfaces

The relevance of this study is determined by the growing requirements for the reliability and durability of machine parts operating under conditions of intensive mechanical loads, elevated temperatures, and exposure to corrosive environments. Modern energy-efficient and environmentally safe surface-hardening technologies, in particular, electrospark alloying (ESA), provide wide opportunities for targeted modification of the structure and properties of surface layers without changing the geometric parameters of products. This paper aims to analyse combined electrospark technologies for forming functional coatings and substantiate methods for improving the ESA process using carbon-containing pastes (special technological environment — STE) and nanostructuring surface layers by adding carbon nanotubes to their composition. The paper presents the results of investigations of the structural–phase composition and service properties of coatings obtained using improved ESA technologies. The methods of electrospark carburizing, ESA with hard wear-resistant and soft antifriction metals, the formation of combined multilayer coatings, as well as hybrid technologies combining ESA with subsequent surface plastic deformation (SPD), are considered. Microstructural,

Citation: V.B. Tarelnyk, O.P. Haponova, N.V. Tarelnyk, Ie.V. Konoplianchenko, M. A. Mikulina, and V.V. Postolatii, Improving the Quality Parameters of Steel Surfaces by Combined Electrospark Carburizing Technologies. Pt. 1. Properties of Metal Surfaces, *Progress in Physics of Metals*, **27**, No. 2: 304–346 (2026)

tribological, and mechanical tests are carried out along with an analysis of the stress–strain state of surface layers. The obtained results show that electrospark carburizing provides an abnormally high diffusion of carbon and the formation of nonequilibrium fine-grained structures with hardness up to 72 *HRC*. The combination of ESA using a graphite electrode followed by SPD makes it possible to reduce surface roughness to R_a = 0.1–1.5 μm, increase wear resistance and adhesion strength of the coatings, and control the level of residual stresses. The use of STE containing carbon nanotubes promotes the formation of nanostructured coatings with increased microhardness and corrosion resistance. The practical application of the obtained results consists of the implementation of combined electrospark technologies for strengthening and restoring machine parts, in particular, components of pumps, seals, and bearing units that ensures increased reliability and durability.

Keywords: electrospark alloying, electrospark carburizing, combined coatings, microstructure, durability of machine parts.

1. Introduction

The main driving force of long-term economic growth is scientific and technological progress, which is inextricably linked with the emergence of new, more reliable technologies, which are characterised by environmental safety, lower material and energy costs, and extended service life. At the same time, a large number of modern machines and mechanisms have to work under conditions of corrosive, abrasive, adhesive and other types of influence of working environments destroying the surfaces of the parts [1–3]. In addition, the surface layers of the parts are negatively affected by increased operating modes of the equipment, namely: high speeds, loads, and contrasting temperatures [4, 5].

The modern technologies for improving the quality of the part surface layers include a significant number of strengthening methods aimed at protecting the part surfaces from wear. Among such methods, chemical-thermal treatment (CTT) has become the most widespread one [6–8]. Increased hardness and wear resistance of part surfaces can also be achieved through gas-thermal spraying of metal-ceramic coatings [9], micro-arc oxidation [10], centrifugal reinforcement with tungsten carbide [11], application of aluminium oxide layers [12–14], as well as the use of plasma and detonation spraying methods [15–19], magnetron spraying [20–22], *etc*. In addition, there are technologies aimed at improving the operational properties of surfaces at the design stage by ensuring the required geometry of the surface layer of the product (research on centrifugal dispersing devices, gravitational transport, cylindrical surfaces of parts [23, 24].

Increasing the surface wear resistance is also achieved by applying the multilayer coatings [25] that combine the features of hard wear-resistant materials and soft antifriction ones [26–28]. The technological solutions are aimed at optimising the structure and properties of such coatings

while ensuring their high adhesion strength, as well as forming the necessary tribotechnical characteristics, which increase the durability of the parts under difficult operating conditions.

Thus, the technological developments aimed at creating the modern composite materials with a stably increased wear resistance of the surfaces, as well as relatively high strength and viscosity, are relevant and timely [6, 29–31].

A modern solution directed to the problem of creating energy-efficient and low-cost technologies for improving the quality parameters of the part surface layers is the treatment of the materials with the use of concentrated energy flows (CEF). Among such methods, the most widespread are ion nitriding [32, 33], condensed ion bombarding [33–35], plasma spraying [36–39] and plasma treating [40, 41], as well as laser processing [42–45].

The most popular modern technology implemented using the CEF is the electrospark alloying (ESA) method, due to which structures having unique physical-mechanical and tribological properties at the nanoscale are formed in the surface layers [46]. In works [47, 48], the ESA process is presented that occurs between the surface layers of the anode (alloying electrode) and the cathode (part), which are subject to the local action of high shock wave pressures and temperatures. While approaching one another, the surfaces of the electrodes (anode and cathode) in microscopically small volumes are almost instantaneously (for 50 to 400 microseconds) heated to temperatures of $(5–7)\times10^3$ K. After that, the heated fragments in the form of drops or solid particles of the anode material start moving to the cathode surface. At this moment, on the cathode surface, there occur the microbaths, wherein the anode and cathode materials are interacting with each other and with the environment. The high temperature activates diffusion processes, causes a change in the structure of the surface layer and results in the formation of new phases.

The features that favourably distinguish the ESA method from the traditional surface treatment technologies include: environmental and technogenic safety; the ability to form the coatings consisting of pure metals, the alloys of any degree of alloying, hard alloys, cermet, *etc.*; application in local areas that require no protection of adjacent surfaces; high adhesion of the deposited metal; due to the diffusion of the elements of the alloying electrode-tool (ET) into the surface layers of the part, the ability to control the structure of the surface without changing the geometric dimensions; the absence of warps and deformations; the possibility of integration into any technological process; small size and transportability of the ESA equipment, *etc.* [49, 50]. Additionally, in [51], it has been shown and proved that the ESA method is one of the most suitable for applying discrete coatings, since the process itself is discrete in nature. The advantage of such coatings is the absence of a softening effect during the propagation of a brittle crack spread from the coating to the base

metal, which is due to the excessively high adhesion strength within the continuous layers. The high cohesive and adhesive stabilities of the individual discrete coating elements are achieved by limiting the normal stresses in the coating itself and the tangential stresses in the plane of the adhesive contact with the base, which is implemented by selecting the sizes and shapes of the discrete areas. The principle of the discrete structure of the coatings has made it possible to combine organically the physical processes underlying the pulse hardening methods with the structural discreteness that determines the operational properties.

The disadvantages of the ESA method include the availability of increased surface roughness, reduced fatigue strength and other factors [52, 53]. However, some of them can be considered advantages. In particular, for a number of the technologies for strengthening and restoring the parts, it is necessary to ensure the increased adhesion of the coating to the substrate, which is achieved by creating rough surfaces thereof [54]. The protrusions and depressions of the roughness, which is formed by traditional mechanical processing methods (turning, grinding, *etc.*), have a pointed profile, resulting in the appearance of stress concentrators and, accordingly, the decrease in fatigue strength. After surface treatment by the electro-spark alloying method, the resulting roughness is characterised by a gently sloping profile without sharp drops in the surface 'landscape' [55]. Such surface morphology enables the effective application of electro-spark alloying as part of a combined technology, for example, electro-spark alloying followed by the application of a metal-polymer material (ESA + MPM) [56].

Depending on the ESA method, the alloying medium, and the cathode and anode material, the properties of the surface layers are sufficiently presented in [27, 57–61].

With the appearance of new technologies, improving the quality parameters of machine parts surfaces by the ESA methods, which use the special technological saturating media (STSM), has significantly expanded the range of their application. It has become possible to obtain the surface structures having unique physical-mechanical and tribological properties at the nanoscale. At the ESA process, using the STSM, it is possible to obtain not only the single-component coatings, namely, aluminising [51, 62], carburizing [63–65], nitriding [66], but also the multi-component ones [67, 68].

The wide opportunities for the targeted changes in the properties of the metal surfaces were opened when using graphite as an anode during the ESA process. According to Ref. [69], the choice of graphite as an electrode material has been justified by a number of its advantages. It is known that graphite in the free state is an effective solid lubricant, and in the bound state, in the form of carbides, it acts as a solid wear-resistant phase, which is resistant to the action of many aggressive environments [70]. In some events, the combination of these properties is necessary.

When the ESA method is carried out using a graphite electrode, it is based on the diffusion process, namely, the process of saturation of the surface of the part with carbon. This is not accompanied by an increase in the size of the part; the surface is saturated with carbon due to diffusion, which gives a reason to compare it with a type of CTT, namely, carburizing.

During the ESA process, strengthening of the surface of the part occurs due to diffusion-hardening processes. The surface of the part is saturated with carbon at a high temperature (up to 10,000 °C), after which it is rapidly cooled to room temperature.

In Ref. [71], the authors have investigated the process of electric spark carburizing (ESC) of steel surfaces. This process has a number of advantages compared to the traditional methods used when applying the ESA method. The main advantages of the ESC method are as follows: achieving 100% continuity of the strengthened surface, increasing the hardness of the surface layer of the part due to the diffusion strengthening processes, the possibility of local processing (alloying can be carried out in certain places without protecting the rest of the part surface), *etc.* During the ESC process, the discharge energy in the range from 0.036 to 6.8 J and the process productivity in the range from 0.5 to 3.0 cm^2/min are used.

In Ref. [72], the modern scientific research in the field of processing metal surfaces with a graphite electrode during the ESA method was reviewed and analysed. The authors have studied the influence of the parameters of the electric pulse on the quality of the carburised layer. The microstructural analysis showed that three characteristic zones can be distinguished in the structure of the layer, namely, the carburised ('white') layer, the diffusion transition zone and the base metal zone. The authors have substantiated the need for non-abrasive ultrasonic finishing (NAUF) after the ESC process in order to reduce the surface roughness, change tensile stresses to compressive ones and increase the fatigue strength of the parts. In addition, to reduce the roughness of the treated surface, it has been proposed to apply the ESC technology in stages, with a reduction in the discharge energy (W_p) at each subsequent stage. To improve the quality parameters of the carburised layer obtained using the ESC process, it has been proposed to use graphite powder, which had been applied to the treated surface before alloying.

The comparative analysis has shown that after the traditional ESC process at $W_p = 4.6$ J, the surface roughness of steel 20 is $R_a = 8.3–9.0$ μm, and after using the proposed technology, it is $R_a = 3.2–4.8$ μm. At the same time, the continuity of the alloyed layer increases up to 100%, the depth of the carbon diffusion zone increases up to 80 μm, as well as the microhardness of the 'white' layer and its thickness increase up to 9932 MPa and 230 μm, respectively. The local micro-x-ray spectral analysis of the obtained coatings has shown that the traditional ESA method at $W_p = 0.9$,

2.6, 4.6 J provides the formation of surface layers having high carbon contents with a depth of 70, 100, 120 μm, respectively, and the ESA method using graphite powder ensures those with a depth of 80, 120, 170 μm, respectively. With increasing the depth, the amounts of carbon decrease from 0.72 to 0.86% to those in the base metal from 0.17 to 0.24%. In the subsurface layer, which has been formed using the new technology, the pores are filled with free graphite, which can be used as a solid lubricant to improve the performance characteristics of the friction pair parts processed by it. Statistical thermodynamics and ordering kinetics models developed to describe the evolution of long-range order and phase transformations in alloys can be used as a theoretical basis for analysing structural changes and improving the quality parameters of steel surfaces during ESA [73].

Considering that the ESA method with a graphite electrode has a wide range of applications, the analysis of modern scientific research in the field of metal surface treatment by the electrospark carburizing method does not provide a complete picture of its other possibilities. The formulation of the purpose of the work determines the importance of conducting further research.

The purpose of this work focuses on the following aspects:

- analysis of the properties of metal surface coatings formed by the ESC method;
- investigation of the properties of metal surface coatings formed by the ESA method from hard wear-resistant or soft antifriction metals, taking into account the sequence of the ESA process (before or after the ESA treatment);
- improving the quality parameters of the surfaces formed by the ESC method;
- analysis of the stress–strain state of the surface layers after the ESC method and after a combination of the ESC process with the ESA method using soft antifriction metals;
- assessment of the influence of a special technological environment (STE) with uniformly distributed carbon nanotubes on the modification of the surface layers of the machine parts formed by the ESA method.

2. The ESC Method for Increasing the Hardness of Metal Surfaces

To increase the hardness of steel parts, the method of electrospark carburizing has been proposed. When strengthening the parts made of rolled steel sheets, the method provides environmental safety thereof [74]. The method involves treating the steel surfaces with temperatures characteristic of hardening and tempering processes for parts having a thickness of 1.0 to 10 mm. In this case, the values of the energy discharges (W_p) in the range of 4.6 to 6.8 J and processing productivity of 0.2 to 3.0 cm^2/min are used.

Owing to the ESA treating the steel surface with a graphite electrode, the following processes occur:

• saturating the steel surfaces with carbon, and due to concentrated energy flows, providing abnormally high diffusion of carbon, which is observed, while the carbon content in the surface layer can be of 3 to 4% [75];

• performing ultra-high-speed hardening with the use of short-term heating by an electric current discharge to a high temperature, and then instantaneously cooling, which leads to the formation of non-equilibrium structures having fine grains, high heterogeneity in composition, structure, and a high level of thermal stresses;

• providing the plastic deformation under the local action of pulse pressure on the material.

The listed processes affect the formation of the properties of the obtained surface layers. Table 1 presents the results of measuring the hardness of rolled steel sheets made of 65Г (65G), 40Х (40Kh) and 30Х13 (30Kh13) after the ESC process and heat treatment: (1) ESC processing and cooling in the air, (2) ESC processing and cooling in oil.

Table 1. **Technological parameters of the surfaces of steel sheet samples strengthened by the ESC method [75]**

Sample thickness, mm	Discharge energy W_p, J, hardening/tempering	Productivity, cm/min, hardening/tempering	Hardness, *HRC*, sample ESA side (Air cooling)	Hardness, *HRC*, sample reverse side (Air cooling)	Hardness, *HRC*, sample ESA side (Oil cooling)	Hardness, *HRC*, sample reverse side (Oil cooling)	Roughness R_a, μm
Steel 65Г (65G) (rolled sheet, according to ГОСТ 19903-74 (GOST 19903-74)							
1	4.6/4.6	0.3/1.0	69/69	55/55	72/71	69/67	3.7
2	6.8/4.6	3.0/0.7	69/69	53/53	72/71	67/65	4.1
3	6.8/6.8	2.0/3.0	68/68	45/44	71/70	66/62	4.3
4	6.8/6.8	1.5/2.4	66/66	43/43	70/69	64/60	4.5
5	6.8/6.8	1.4/3.0	63/63	41/41	70/68	62/60	4.9
6	6.8/6.8	1.0/2.0	62/62	40/40	70/67	62/60	5.2
7	6.8/6.8	0.7/1.0	60/60	38/38	69/65	61/60	5.1
8	6.8/6.8	0.5/0.7	60/60	37/37	69/64	61/60	5.5
9	6.8/6.8	0.3/0.6	59/59	35/35	65/62	61/60	6.7
10	6.8/6.8	0.2/0.4	59/59	33/33	63/59	61/59	6.8
Steel 30Х13 (30Kh13) (rolled sheet, according to ГОСТ 5582-75 (GOST 5582-75)							
4.0	6.8/6.8	1.5/2.4	65/64	42/40	67/65	60/59	4.3
Steel 40Х (40Kh) (rolled sheet, according to ГОСТ 19903-74 (GOST 19903-74)							
5.0	6.8/6.8	1.4/3.0	63/62	38/34	65/61	50/48	5.1

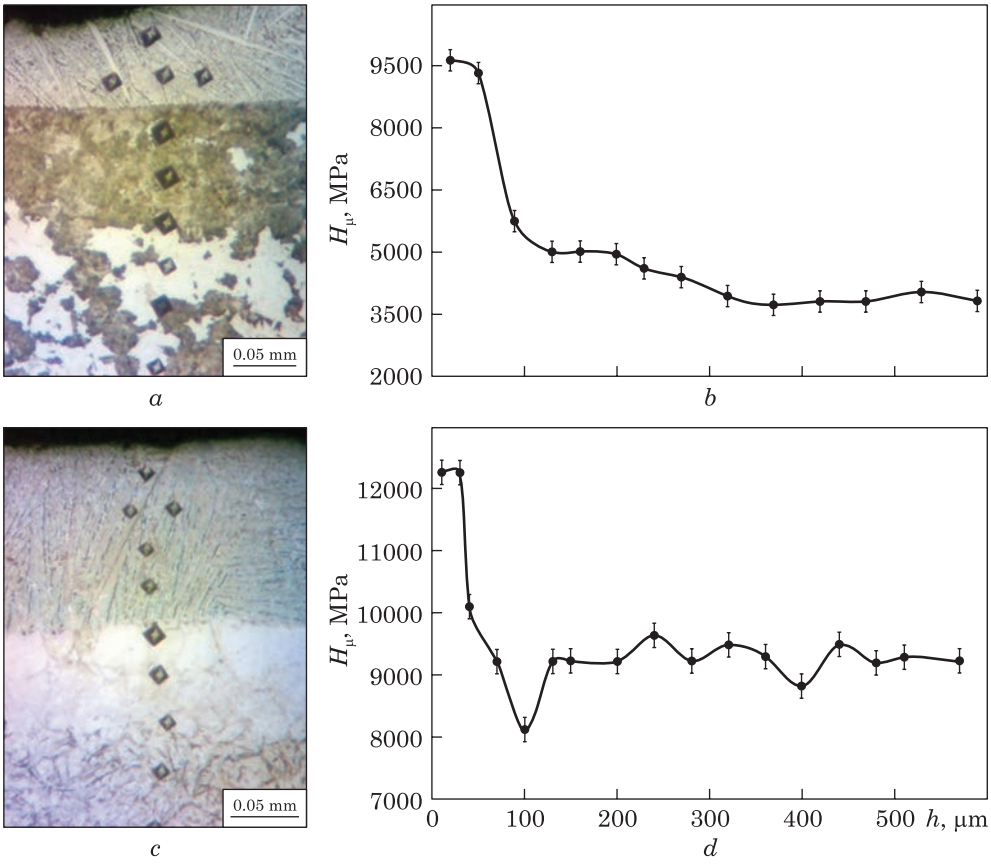

Fig. 1. Microstructure (*a*, *c*) and microhardness distribution (*b*, *d*) in 65Г (65G) steel samples of 3 mm thick after ESC processing and air cooling (*a*, *b*), and those of 2 mm thick after the ESC processing and oil cooling (*c*, *d*) [75]

Due to the above processes occurring during the ESC method, it is possible to achieve a hardness of up to 72 *HRC* on the surface being carburised, and up to 69 *HRC* on the reverse side of the thin sheet blank, as seen in Table 1.

The results of the metallographic and durometric analyses confirm the formation of non-equilibrium structures having an increased hardness after the ESC process. Figures 1, *a* and *b*, respectively, show the microstructure and microhardness distribution depending on the depth, starting from the surface, of the 3 mm thick 65Г (65G), steel sample after ESC processing and air-cooling. The maximum microhardness, reaching 9500 MPa, is observed on the alloyed surface of the sample. With increasing depth, the microhardness decreases; at a depth of 300 μm, it is 4000 to 4500 MPa, and then it changes slightly over the entire cross section.

Figures 1, *c* and *d* show the microstructure and microhardness distribution as the depth increases from the surface of the 2 mm thick 65Г (65G) steel sample after ESC processing and oil cooling. The maximum microhardness value of 12500 MPa is on the alloyed surface of the sample. With increasing depth, the microhardness has been decreasing. At a depth of 80 to 120 μm, there is a drop in microhardness up to 8000 MPa. After that, the microhardness value has been increasing up to the value of 9100 to 9600 MPa, and then it does not change throughout the cross section.

Thus, a new, environmentally safe technology for the heat treatment of the parts made of the rolled steel sheets, namely, steels 40Х (40Kh), 65 Г (65G), and 30Х13 (30Kh13) (pump blades, screws, disks, *etc.*), is proposed for practical application.

3. Using the ESC Method to Increase the Thickness of the Strengthened Layer

Before applying the hard wear-resistant metals, ESC processing the metal surfaces had been performed in order to increase the thickness of the elevated hardness layer. For example, in works [33, 76–80], to increase the wear resistance of the working surfaces of the steel rings for the pulse end seals (PESs), the multilayer combined electrospark coatings (CESCs), which had been formed in the sequence of ВК8 (VK8) + Cu + + ВК8 (VK8), were used. Before applying the CESCs, the working surfaces of the steel rings were treated by the ESC method using the discharge energy W_p in the range of 0.036 to 4.6 J, while the thickness of the increased hardness layer was increased by the value of the thickness formed by the ESC method.

The improved parameters of the working surfaces of the steel rings for the PESs have a positive effect on their wear resistance.

4. The ESC Method for Reducing the Hardness of Metal Surfaces

In the literature, practically, there is no information on the use of the ESA method to reduce the hardness of the surface layer of the parts. However, the technologists are often faced with such a problem. When assembling the stationary component parts, in addition to ensuring the strength of the connections, there is often a problem of ensuring the connection tightness, for example, in the seats of the metal rings for the pulse end seals (PESs).

While assembling the stationary component part connections, the part surfaces being connected are subject to plastic deformation; therefore, it is desirable that the hard metal parts have a softer surface layer.

The hardness of the metal surface of the part can be regulated as follows [81]:

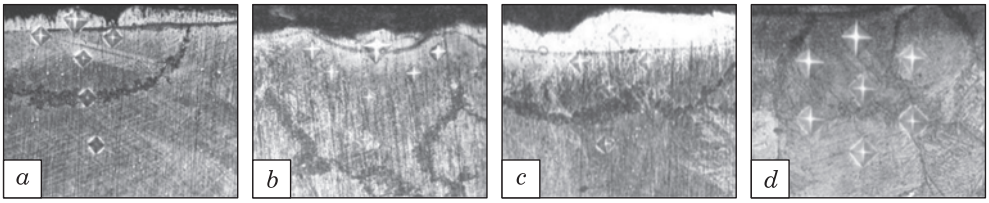

Fig. 2. The microstructure of the BrB2 surface layer after the ESC method with carbon for (*a*) 1 min, (*b*) 2 mins, (*c*) 3 mins, (*d*) 4 mins; ×400 [81]

Table 2. **Hardness distribution and depth of the БрБ2 (BrB2) surface layer [81]**

Electrode-tool (ET) material	Strength, *N*, W	Labour intensity, min/cm^2	Depth of the low-rigidity layer, μm	Hardness distribution, *HV*, over depth
Carbon	144.3	1.0	25	145, 195, 312, 370
Carbon	144.3	2.0	30	140, 260, 280, 370
Carbon	144.3	3.0	50	184, 195, 220, 370
Carbon	144.3	4.0	120	229, 250, 260, 370

• increasing the hardness by applying a material with a higher hardness to the surface or diffusively introducing the necessary chemical elements from the environment or anode material;

• reducing the hardness by applying softer materials to the surface.

When using this method for processing the surfaces of the parts being connected, sufficient tightness, strength and reliability of the stationary component part connections are not always achieved. The problem is solved by treating the surface of the steel cathode by the ESC method at W_p = = 0.4–4.0 J, which leads to the formation of a surface 'white' layer, the hardness of which exceeds the hardness of the base steel, and a sublayer, namely, a tempering zone located under the surface 'white' layer and characterized by a hardness that is lower than the hardness of the base metal. After conducting the ESC process, the surface 'white' layer is removed, for example, by grinding [82].

In the other variant, a cathode made of a non-ferrous alloy is used. In this case, the surface of the cathode is treated by the ESC method at W_p = 0.4–4.0 J with the formation of the surface tempering zone, the hardness of which is lower than the hardness of the base non-ferrous metal. Moreover, with an increase in the charge energy and the alloying time, the depth of the reduced hardness layer increases.

From the analysis of the microstructures in Fig. 2 and the data in Table 2, it follows that with an increase in the alloying time from 1 to 4 min/cm^2, the depth of the hardened layer increases from 25 to 120 μm. The hardness value also increases from 140 to 229 MPa.

When used for processing the surfaces of the parts being connected, to obtain their stationary component part connections characterised by in-

creased tightness and strength, the proposed ESC method [82] allows obtaining the stationary component part connections with improved values of tightness and strength and, as a result, increasing their reliability and durability.

5. The ESC Method for Reducing the Surface Roughness after the ESA Process with Soft Antifriction Alloys

When developing a new method for applying combined electrospark coatings (CESCs) made of the soft antifriction metals to the steel liners of plain bearings (PL), the above problem arose of reducing their roughness. To solve this problem, the following ESC method was used.

Traditionally, the babbitt alloys are applied to the base of the PL liners using various processing methods, including manual pouring, centrifugal pouring, pressure-assisted pouring, gas-thermal spraying, *etc.* [83]. In recent years, to apply the antifriction coatings, the ESA method has been increasingly used.

The closest method to the proposed one is tinning the liners and pouring an antifriction alloy of the soft metals into a chill mould onto the liners heated to 250 °C under pressure and at the temperature of 450 to 480 °C.

Before pouring the antifriction alloy onto the surface to be poured, using the ESA method performed by the electrode-tool (ET) made of copper, the intermediate layer had been applied onto the surface to be poured. While tinning, copper with tin could form a solid substitution solution, providing a guaranteed metallic bond [53, 84].

It should be noted that not all methods for controlling the process of babbitt pouring can give a full guarantee of its quality.

6. Combined Copper and Babbitt Electrospark Coating Made on a Steel Substrate

To ensure the high-performance characteristics of the part surfaces, it is important to obtain a coating with maximum continuity and minimum roughness. For this purpose, alloying by copper was carried out in stages [85]: first at W_p = 0.27 J, and then at W_p = 0.05 J. It resulted in decreasing both the layer thickness from 0.08 to 0.05 mm and the roughness (R_a) from 10.4 to 6.2 μm. The layer continuity reached 100% in Fig. 3, *a*.

At the second stage, when applying copper at a lower energy mode, the electric discharges were localised on the protrusions of the previous layer, which eventually led to their partial destruction and deformation. This contributed to a reduction in the surface roughness and an increase in its continuity.

Next, babbitt B88 (B88) was applied to the copper coating. The process for forming the babbitt layer was also carried out in stages. First, the mode was used at W_p = 0.05 J, and then at W_p = 0.27 J.

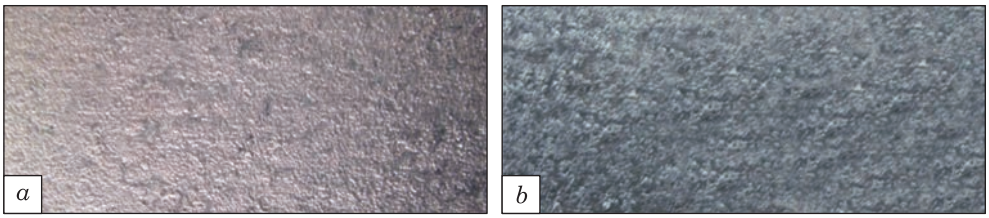

Fig. 3. The sample made of steel 20 after the ESA process by copper (*a*) and copper and babbitt (*b*) [85]

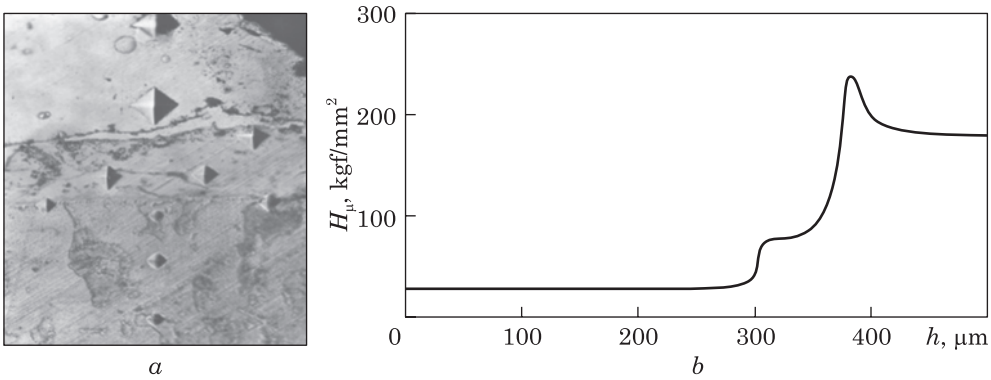

Fig. 4. The structure of the babbitt coating with the copper sublayer (*a*), and the distribution of the microhardness by the depth of the formed layer (*b*) on the sample made of steel 20; ×400 [85]

It should be noted that when applying tin babbitt to a copper surface at discharge energy of more than 0.05 J, the quality of the coating decreases sharply (the continuity decreases and the roughness increases). Babbitt is transferred in the form of separate drops, and the higher the discharge energy, the larger the droplet sizes and the lower the continuity of the coating.

The initially applied babbitt layer at pulse energy of W_p = 0.05 J accumulates the heat and increases the time for the drop to spread when applying the next babbitt layer at a higher alloying mode. Figure 3*b* shows the surface of the sample after the ESA process by babbitt at W_p = 0.05 J, and further at W_p = 0.27 J. With the increase in pulse energy from 0.05 to 0.27 J, the surface roughness increased from 6.5 to 23 μm, and the thickness of the applied layer increased from 0.08 to 0.42 mm.

Further, to reduce the surface roughness, ESC processing of the coatings was performed at W_p = 0.39 J, and then, at W_p = 0.13 J. Before each treatment with graphite, the coating surface was cleaned with a brush.

During the ESC process, the electric discharges pass along the protrusions of micro-irregularities of the babbitt B88 (B88) surface. This leads to melting, decreasing micro-irregularities in their height, spreading the

Table 3. **The quality parameters and the ESA modes during the formation of the coatings made of tin babbitt having a sublayer of copper, tin bronze, and tin [85]**

Stage number	Electrode tool material	Discharge pulse W_p, J	Productivity, cm²/min	Roughness R_a, μm	Thickness of applied coating, mm
		Steel 20 + Cu + Б88(B88)			
1	Cu	0.27	2.0	10.4	0.08
2	Cu	0.05	1.0	6.2	0.05
3	Б88 (B88)	0.05	1.0	6.5	0.08
4	Б88 (B88)	0.27	2.0	23.0	0.42
5	Graphite	0.39	3.0	16.4	0.38
6	Graphite	0.13	1.3	8.6	0.35
7	Б88 (B88)	0.27	2.0	24.3	0.74
8	Graphite	0.39	3.0	16.7	0.71
9	Graphite	0.13	1.3	9.1	0.70
10	Б88 (B88)	0.27	2.0	23.6	1.04
11	Graphite	0.39	3.0	16.2	1.02
12	Graphite	0.13	1.3	8.7	1.00
		Steel 20 + БрОФ 10-1(BrOF10-1) + Б88(B88)			
1	БрОФ10-1 (BrOF10-1)	0.13	1.3	30.2	0.10
2	БрОФ10-1 (BrOF10-1)	0.05	1.0	7.3	0.05
3	Б88 (B88)	0.05	1.0	6.8	0.08
4	Б88 (B88)	0.27	2.0	23.2	0.45
5	Graphite	0.39	3.0	16.4	0.42
6	Graphite	0.13	1.3	8.6	0.40
7	Б88 (B88)	0.27	2.0	24.6	0.74
8	Graphite	0.39	3.0	16.3	0.71
9	Graphite	0.13	1.3	9.2	0.69
10	Б88 (B88)	0.27	2.0	23.1	1.01
11	Graphite	0.39	3.0	16.8	0.98
12	Graphite	0.13	1.3	8.9	0.97
		Steel 20 + Sn + Б88(B88)			
1	Sn	0.13	1.33	32.7	0.1
2	Sn	0.05	1.0	14.8	0.07
3	Б88 (B88)	0.27	2.0	23.2	0.40
4	Graphite	0.39	3.0	16.8	0.37
5	Graphite	0.13	1.3	8.0	0.35
6	Б88 (B88)	0.27	2.0	24.6	0.71
7	Graphite	0.39	3.0	16.3	0.68
8	Graphite	0.13	1.3	8.2	0.66
9	Б88 (B88)	0.27	2.0	22.1	0.95
10	Graphite	0.39	3.0	15.1	0.92
11	Graphite	0.13	1.3	8.0	0.90

coating material over a larger area, and increasing the continuity of the coating. The total thickness of the coating after the ESA process by babbitt and the subsequent ESC process was 0.35 mm, and the roughness (Ra) was 8.6 μm.

To obtain a thicker layer, the ESA process using the ET made of tin babbitt, which is followed by the ESC process, can be repeated several times, starting with processing with W_p = 0.27 J. After three such procedures, a total coating thickness of up to 1.0 mm can be obtained.

Figure 4, *a* shows the structure of the babbitt coating having a copper sublayer, and Fig. 4, *b* shows the distribution of microhardness over the depth of the formed layer.

The analysis of the structure of the babbitt coating having a copper sublayer has shown that the formed layer consists of 4 zones. The highest layer, which has a thickness of up to 300 μm and microhardness of H_μ = 24–36 kgf/mm^2, is made of babbitt, below there is a layer of copper, the depth of which is 50 μm, and the microhardness is of H_μ = 75–85 kgf/mm^2. Even lower, between copper and steel 20, there is a transition zone having a depth of 10 to 20 μm and microhardness of H_μ = 95–120 kgf/mm^2. Further, with increasing depth, the microhardness has been gradually increasing up to the microhardness of the heat-affected zone (220–240 kgf/mm^2), and then it has been going into the microhardness of the base metal of H_μ = 175–180 kgf/mm^2.

In the same sequence, the babbitt coating, having a transition layer made of tin bronze and tin, is applied.

Table 3 presents the modes of stage-by-stage applying the antifriction coatings made of tin babbitt with a sublayer of copper, tin bronze and tin, as well as the values of layer thickness and surface roughness at each stage of the ESA process.

It should be noted that a significant disadvantage of babbitts is their low fatigue resistance, especially at temperatures above 100 °C. As the thickness of the bearing filler decreases, the fatigue resistance increases, while the minimum thickness of the babbitt filling of 0.25 to 0.4 mm is allowed.

Thus, when applied in a thin layer, the combined electrospark coating (CESC) takes on more load within the permissible working gap of the plain bearing (PB) for the 'liner-shaft' connection. In addition, a thin coating contributes to reducing the cost of the process for manufacturing the bearing liners (BL). The resulting CESC has a minimum thickness of 250 μm and a maximum thickness of 1.0 mm. Further increase in the layer thickness is possible, but not advisable due to an increase in processing time and a decrease in the mechanical strength of babbitt. The bearing liners processed by the proposed method have high reliability and durability during operation, because at all stages of the formation of the antifriction coating, a strong metal bond is ensured both between the base and the intermediate layer of copper, tin bronze or tin, and between those and the

subsequent layer of tin babbitt. The method gives a full guarantee of the high quality of the coatings obtained. It can be used both in manufacturing the new PB liners and in repairing them [86].

7. The ESC-Method-Based Hybrid Technologies

The hybrid technologies based on the ESA method are widely used to improve the quality of the metal part surface layers. To reduce the surface roughness after the ESC process, the method of non-abrasive ultrasonic finishing (NAUF) is usually used in Table 4 [87, 88]. The results of the research on the quality parameters of the surface layer of steels 38XMIOA (38KhMUA) and 40XH2MA (40KhN2MA) after the ESC process and the NAUF are given in Table 4.

The results of reducing the roughness parameters for many machine parts given in Table 4 are insufficient. In this case, the use of grinding after the ESC process is impossible because under such conditions, at least 50–100 μm of the surface layer is removed, and this is the layer portion of the greatest hardness.

The quality of the surface layer of the parts formed by the ESC method can be improved by applying soft antifriction materials thereto, for example, copper, silver, *etc.*, and subsequently performing the NAUF process.

In order to reduce the roughness of the surfaces of the parts being processed, it has been proposed, after the ESC process, to alloy the above-

Table 4. **The results of research on the samples after the ESC process and the NAUF**

Steel grade	Discharge energy at ESC W_p, J	Total depth of the strengthened layer, μm	Maximum surface microhardness, *HV*	Roughness, R_a, μm	
				after ESC	after NAUF
38XMIOA (38KhMUA)	0.1	10	900	0.8–0.9	0.2
	0.31	20	900	0.9–1.0	0.3
	0.53	35	950	1.4–1.7	0.6
	0.9	170	1350	1.6–2.0	0.8
	2.83	215	980	5.7–6.9	1.5
	3.4	230	960	8.3–8.5	2.3
	6.8	370	1010	11.9–14.0	3.2
40XH2MA (40KhN2MA)	0.1	10	900	0.8–0.9	0.2
	0.31	20	900	0.9–1.0	0.3
	0.53	37	800	1.4–1.7	0.6
	0.9	163	760	1.7–2.0	0.9
	2.83	245	1002	5.7–6.7	1.5
	3.4	262	1006	8.6–8.9	2.3
	6.8	380	1070	11.9–14.1	3.2

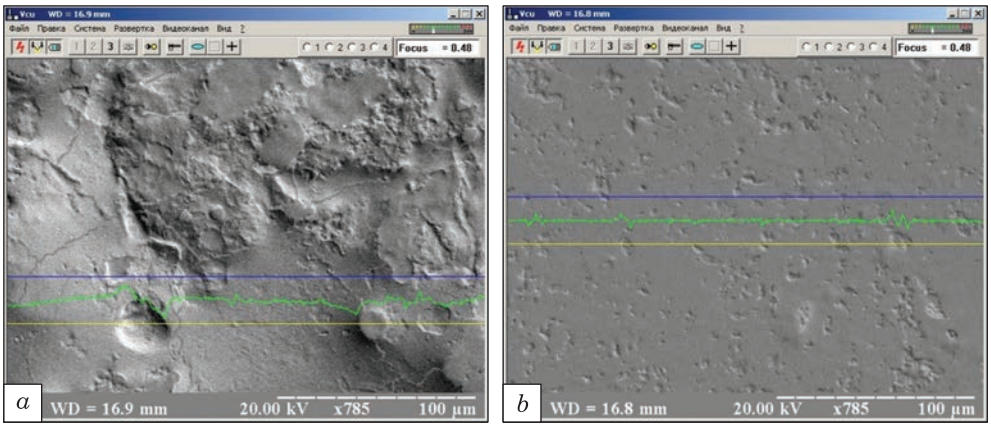

Fig. 5. The surface areas of sample No. 1 (*a*) and sample No. 2 (*b*) [90]

mentioned surfaces by the same electrode, but in stages, with a reduction in the discharge energy at each subsequent stage [89].

The studies were conducted on the flat samples of steel 20 with R_a = = 0.55 mm.

Sample No. 1 was subjected to the ESC process at W_p = 2.83 J. The result of the roughness measurement is R_a = 4.79 mm.

Sample No. 2 was subjected to the ESC process in stages at W_p = 2.83, 0.9 and 0.1 J with the productivity values of 0.5, 2.0, and 2.0 min/cm^2, respectively. The result of the surface roughness measurement is R_a = 1.10 mm.

In [90], the topography and the qualitative characteristics of the surface layer were studied using an electron microscope 'PEM-106 I' ('REM-106 I'). Figure 5 shows the surface areas of samples No. 1 and No. 2 at the same magnification. The images were obtained in a mode that emphasised the surface relief ('Toro' mode). The yellow line describes the base level (0), the blue one indicates the unit of brightness, and the green line demonstrates the contrast distribution along the yellow line. Since the contrast in the image is formed mainly due to the microrelief, the height of the 'teeth' on the green line can be used to estimate the surface microroughness.

Analysing the distribution of microhardness in the samples, one can say that the highest microhardness is determined in the surface layers. For sample No. 1, it is of 920 to 950 *HV* with a propagation depth of up to 60 μm, and for sample No. 2, it is of 690 to 720 *HV* and 30 μm. As the depth increases, the microhardness value for both samples gradually decreases, and at the depths of 130 and 100 μm, it corresponds to the base of microhardness, namely, 180 *HV*.

The decrease in the values of the depth and microhardness of the packed bed for sample No. 2 can be explained by the fact that during the staged ESC process, the discharge energy decreases from W_p = 2.83 to

W_p = 0.9 and W_p = 0.1 J. At the same time, the thermally affected zone decreases, and there occurs tempering, namely, heating the surface layer below the temperature of phase transformation.

Thus, due to the staged carburisation, the roughness of the surface layer is reduced: from R_a = 4.79 to R_a = 1.10 μm; the microhardness in the 'white layer': from 920–950 *HV* to 690–720 *HV*; as well as the total depth of the zone of increased hardness of the surface layer: from 130 to 100 μm.

8. Improving the Quality of the Carburised Layer by Applying the Soft Antifriction Materials

Improving the quality of the carburised layer is one of the important directions for improving the operational properties of the parts treated with the use of the ESA method. One of the effective approaches to the solution of the problem is the implementation of the processes for applying the soft antifriction materials to the surfaces after carburizing thereof. This allows reducing the roughness, improving tribotechnical characteristics and increasing the durability of parts being processed.

The special samples in Fig. 6, made of 40X (40Kh) steel, were used for research. Before the ESC process, the surfaces of the disks were ground to R_a = 0.5 μm. The samples were fixed in the chuck of a lathe, and thereafter the ESC process and the ESA method by the EIs made of silver or copper, and then the NAUF method were carried out.

The results of the study of the following series of samples are presented below:

• the staged ESC process (W_p = 2.83 and 0.9 J with a productivity of 5 and 2.0 min/cm^2, respectively); the NAUF treatment (sample No. 3);

• the ESC process (W_p = 2.83 J; with a productivity of 5 min/cm^2); The ESA method by the EIs made of silver (W_p = 0.4 J with a productivity of 1 min/cm^2); BUFO (sample No. 4);

• the ESC process (W_p = 2.83 J with a productivity of 5 min/cm^2); the ESA method by the EIs made of copper (W_p = 0.4 J with a productivity of 1 min/cm^2); the NAUF treatment (sample No. 5).

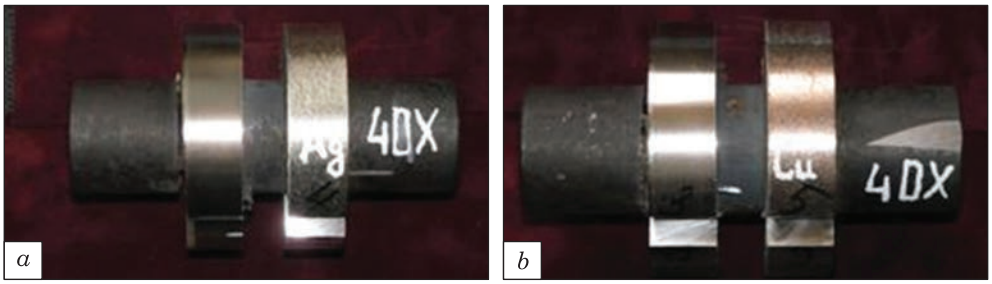

Fig. 6. The samples for the ESC process and the ESA method: silver (*a*) and copper (*b*) [91]

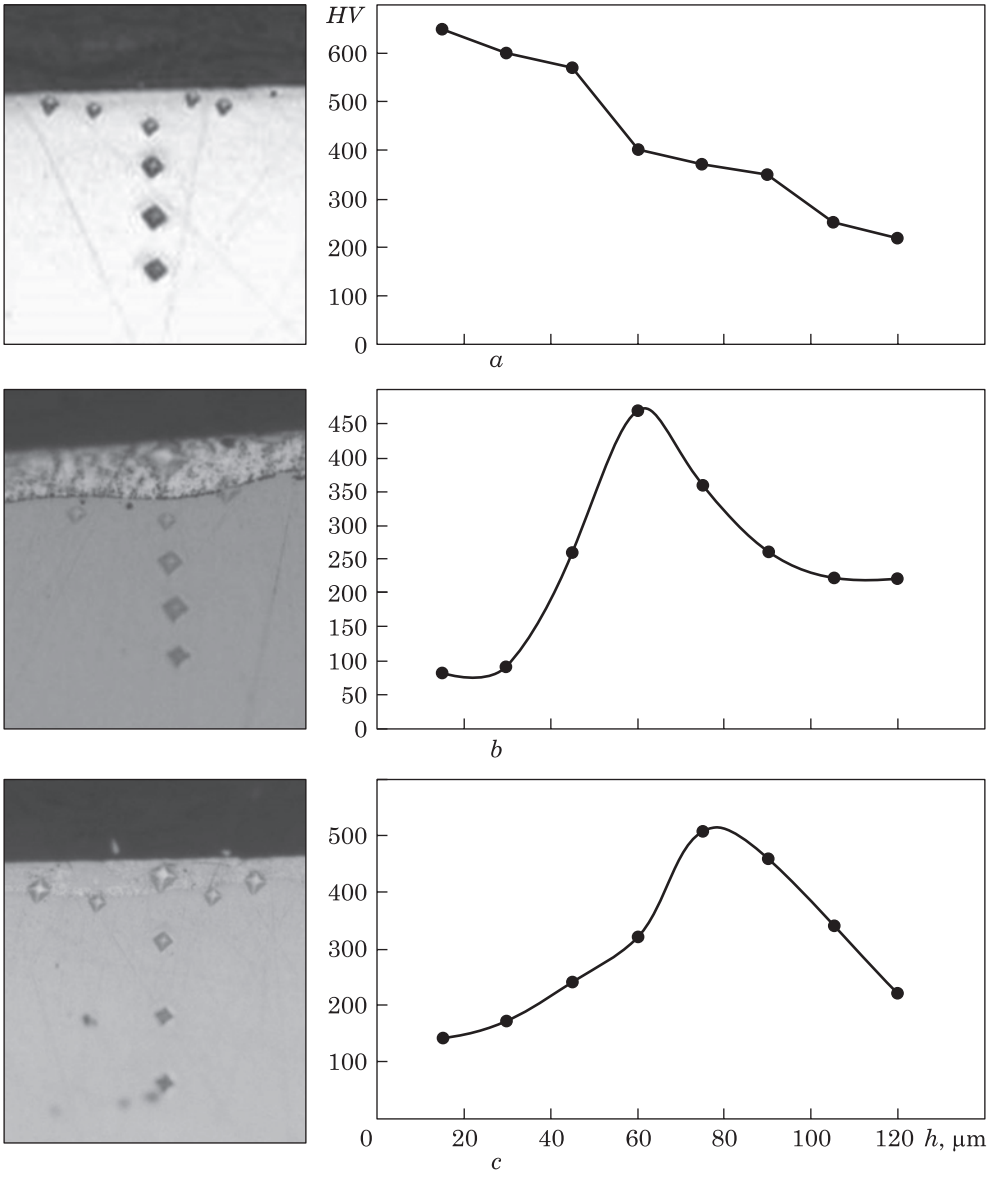

Fig. 7. Microsection (*a*) and hardness distribution in the surface layer of samples No. 3 (*a*), No. 4 (*b*) and No. 5 (*c*) [91]

Due to the NAUF treatment for sample No. 3, the surface roughness decreased from $R_a = 2.30$ to $R_a = 0.56$ μm; for sample No. 4, from $R_a = 2.26$ to $R_a = 0.88$ μm; and for sample No. 5, from $R_a = 3.15$ to $R_a = 0.80$ μm.

Figure 7*a* shows the microsections and the distribution of the hardness of the surface layer of sample No. 3. The maximum hardness (up to 650 *HV*) is located on the surface of the sample, and as it deepens, it

gradually decreases to the hardness of the base, which is 220 *HV*. The depth of the increased hardness zone extends to 100 μm.

On the surface of sample No. 4 in Fig. 7*b*, there is a layer having a hardness of 80–90 *HV* and a depth of up to 35 μm. Further, as the depth increases, the hardness gradually increases, and at a depth of ≈60 μm, it reaches the maximum value of 470 *HV*; after that, it gradually decreases once again to a depth of 100 μm, at which point it corresponds to the hardness of the base.

On the surface of sample No. 5 in Fig. 7*c*, there is a layer having a hardness of 140–170 *HV* and a depth of up to 40 μm. Further, as the depth increases, the hardness has been gradually increasing, and at a depth of ≈75 μm, it reaches the maximum value of 510 *HV*. Thereafter, it has been decreasing again, and at a depth of 120 μm, it corresponds to the hardness of the base.

Thus, to increase the wear resistance of the steel parts, it could be recommended that a combined technology, which includes the staged ESC process for treating the surface layer, followed by the NAUF process. For use in the friction pairs of the parts being processed, before the NAUF process, onto the ESC area of the surface of one of the friction pair parts, a layer of a soft antifriction metal is applied.

Until a certain time, LLC 'TRIZ' (Society for the Implementation of Engineering Tasks) had been manufacturing the protective sleeves (PS) made of steel 38X2MIOA (38Kh2MUA) or 40XH2MA (40KhN2MA), which were treated by the method for carbonitriding in molten salt followed by surface grinding after hot pressing onto the rotor shaft. However, it should be noted that in this case, a significant portion of the surface layer of the highest hardness was removed, which reduced the effectiveness of this technology.

As an alternative, a new strengthening method was proposed, wherein the heat-treated parts were subjected to the ESC process in combination with the method for ion nitriding (IN). These events were carried out before or after the alloying process, for the time being, sufficient to saturate the metal with nitrogen at the depth of the heat-affected zone [90].

The developed technologies have been widely used by the TRIZ Company in Sumy, Ukraine, to improve the quality of the elements of the floating sealing assemble units for centrifugal compressors in Fig. 8. Thus, when repairing the compressors for the Anastasivka CS, the Ukrnafta, the LLC NJSC Azot OSTCHEM Cherkasy 'AZOT', the protective sleeves (PS) were made of 40XH2MA (40KhN2MA) steel, and the IN process thereof was carried out together with a 'witness' sample, whereon the depth and microhardness of the strengthened layer were controlled.

The outer surface of the sleeve, after grinding and pressing onto the shaft, was subjected to a combined process of strengthening by the ESC process followed by the NAUF method.

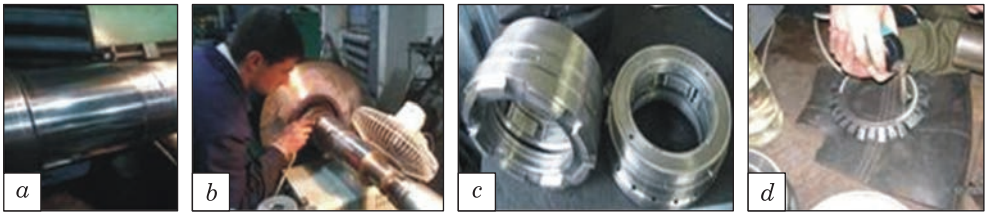

Fig. 8. Application of ESC and ESA technologies in the floating seal of the LLC TRIZ®: (*a*) the PS pressed onto the shaft; (*b*) ESC processing the PS surface; (*c*) floating seal; (*d*) ESC + ESA processing by silver of the floating seal ring [91]

Similarly, the end surfaces of the outer and inner floating rings have been strengthened while manufacturing the outer and inner floating rings. Using the ESA method, copper had been applied to the inner cylindrical surfaces of the floating seals before tinning hereof. After the ESC process, the layer of silver was applied to the contact end surfaces of the sealing rings and the corresponding parts of the housing and cover.

Since 2004 to the present, more than 100 compressor housings have been put into operation. To improve the quality of the floating seal elements, there were used the ESA technologies.

9. The Stress–Strain State of the Surface Layers after the ESC Process and the Hybrid Technology

Surface layer plastic deformation (PD) is an effective method for improving the operational properties of the parts, in particular, their strength, wear resistance, and fatigue resistance. The combination of the ESA process with the PD one, *i.e.*, using the hybrid technology of ESA + PD, is of particular interest, since these processes mutually strengthen each other. The ESA process forms an alloyed and strengthened surface layer, and the PD one optimises its stress–strain state, while reducing the concentration of residual stresses thereof, as well as contributing to reducing the roughness, and improving the tribotechnical characteristics, *etc.* Among the PD methods, special attention is paid to ball rolling (BR) and non-abrasive ultrasonic finishing (NAUF), which make it possible to modify the surface microstructure uniformly, provide for controlling and monitoring the distribution of the internal stresses in the surface layer in Fig. 9.

In Ref. [92], the results of the PD process's influence on the coatings applied by the ET made of hard wear-resistant and soft antifriction materials are presented. When ESA processing is performed by both hard wear-resistant and soft antifriction materials, with the exception of the ESC process, the thickness of the product increases by the thickness of the formed layer.

At ESC processing, the thickness of the product does not change, and in this case, the strengthened, so-called 'white' layer appears on its sur-

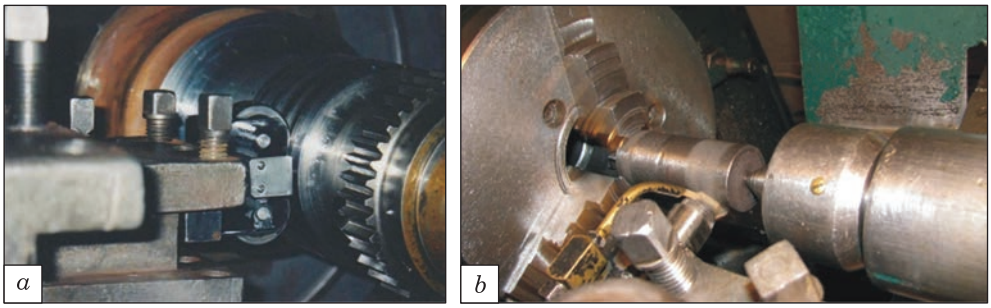

Fig. 9. ESC surface layer treatment: (*a*) ball rolling (BR), (*b*) non-abrasive ultrasonic finishing (NAUF) [92]

face. Its hardness significantly exceeds the hardness of the base. Under the 'white' layer, there is a transition zone, namely, a sublayer, which is a region of the thermal influence of the pulse discharges and the diffusion penetration of the anode elements into the cathode. The hardness of this zone has been gradually changing along the depth of the penetration as compared to the hardness of the 'white' layer.

The analysis of PD methods for processing the surface layers after ESC treatment used either without or with subsequent application of soft antifriction coatings would provide a general picture of the feasibility of implementing the complex of strengthening technologies under consideration. Moreover, it could serve as a reserve to improve the quality of the product surface layers. Thus, there is a need to analyse the stress–strain state (SSS) for the ESC layers, as well as the carburised layers coated by the soft antifriction materials subjected to the PD process.

Below is a methodology being considered to calculate the geometric parameters of the deformation centre for surface layers with complex structures obtained during ESC processing of metal substrates, as well as for carburised layers coated with soft antifriction materials. The above methodology has been developed based on calculating the main geometric parameters of the deformation centre for homogeneous bodies, namely, the engineering method by M.S. Drozd, and grounded on the concept of plastically hardness (*HD*) [93]. The transition from the concept of the hardness of *HB*, namely, a parameter characterising the metal resistance to contact loading, to the concept of the plastically hardness of *HD*, namely, a parameter which is interpreted as a modulus of strengthening the material, allows considering this value as a characteristic of the material resistance to the contact plastic deformation.

The presented method is based on the calculation of the main geometric properties of the deformation centre for homogeneous bodies (engineering method by M.S. Drozd) and is based on the concept of plastically hardness (*HD*). Having compared the plastic hardness of *HD* with the

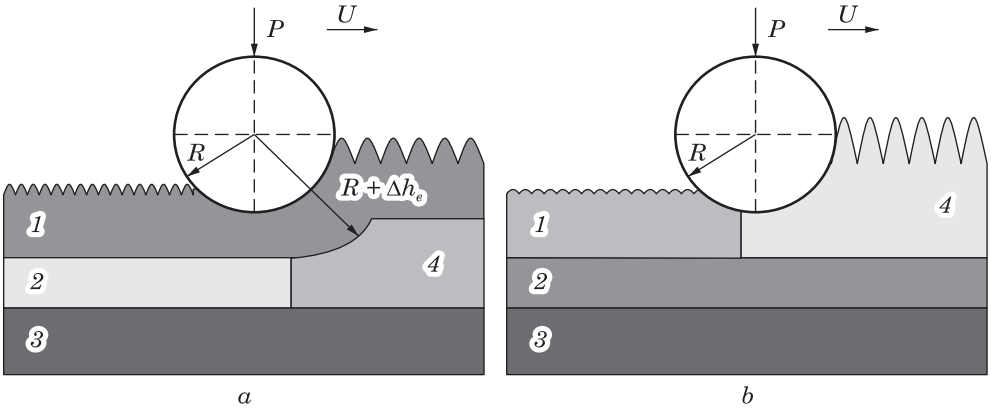

Fig. 10. Surface layer PD scheme: (*a*) ESC (*1* — hard carburised layer, *2* — soft strengthened transition sublayer, *3* — base metal, *4* — non-strengthened transition layer); (*b*) the layer made of soft antifriction metals applied onto the ESC surface layer (*1* — soft strengthened surface layer, *2* — ESC layer, *3* — base metal, *4* — soft non-strengthened surface layer) [92]

Brinell hardness, the following dependence [92] has been obtained:

$$HD = \frac{P - P_0}{\pi D h}, \tag{1}$$

where P is an arbitrary load, P_0 is a critical load equal to the segment cut off by a linear approximation of the function $P = f(h)$ on the P axis; D is the diameter of the inserted ball, and h is the depth of the residual dent.

When replacing the hardness of HB, which determines the metal resistance to contact loading, with the plastically hardness of HD, which is defined as a modulus of strengthening the surface layer material, it allows considering it as a characteristic of the material's resistance to contact plastic deformation. It should be noted that during the PD treatment of the formed ESA layers, such an interpretation of their physical and mechanical properties is more justified and reliably determines the ability of the layer to strengthen during the PD process and, thus, the changes in the operational properties of the surface layer.

Thus, improving the quality of the ESC layers by the PD method (reducing roughness, increasing microhardness, *etc.*) largely depends on the structure of the alloyed layer and on the correctly selected modes of the force influence thereon.

Recently, improving the quality of the surface layers of the rotor shaft bearing journals has become increasingly used by the ESC method, subsequently followed by PD processing [72].

Let us consider the change in the geometric parameters of the contacting bodies depending on the microhardness of the surface layers formed by the ESA method in Fig. 10.

Below, the geometric parameters of the contacting bodies are corrected, taking into account the parameter of the thickness of the hard carburised layer ($\Delta h_c = \Delta h_т$) and the thickness of the soft antifriction metal layer (Δh_c).

At PD processing the carburised surface layer, the indenter in Fig. 10, *a*, under the influence of the load *P* applied thereto, indents the hard carburised layer ($\Delta h_т$) into the softer transitional sublayer while strengthening the latter. The carburised layer increases the radius of the indenter R_i by the value equal to $\Delta h_т$, and reduces the shaft diameter by the value equal to $2\Delta h_т$. The thickness of the carburised layer can be determined according to [94] or by measuring it using the cross-section of the witness sample.

In the event of ESA processing the surface layer by the soft antifriction materials after the ESC process, the microhardness of the surface layer decreases, thereby changing the mechanism of strengthening the surface layer. After ESA processing with the use of the soft metals, the shaft diameter increases by $2\Delta h_c$. In this case, the indenter radius does not change. The soft surface layer is deformed and strengthened, and the transitional layer, being in this case a carburised one, is not strengthened in Fig. 10, *b*.

The stress–strain state (SSS) analysis of the surface layers after the ESC and the ESC + ESA methods by the soft metals and following them the surface PD (plastic deformation) method, as well as the algorithm for calculating the geometric parameters of the deformation centre, as given in Ref. [93], allow determining the geometric parameters of the deformation centre, the depth of the riveted layer, h_s, and the deformation intensity ε_{i0}.

10. Modifying the Part Surface Layers by the ESA Method Using the Special Technological Environment with Carbon Nanotubes

A reserve for solving the problems according to the development of technologies for obtaining the coatings having unique properties, which have increased the values of wear resistance, durability, corrosion resistance, *etc.*, is nanostructuring the product surfaces with the use of various methods. Part surface nanostructures have unique features associated with improving both physical and mechanical properties of the material, which is very important for various branches of science and technology.

The development of new methods for strengthening the surfaces of the parts by the nanostructuring process, which is an environmentally friendly and energy-efficient process based on the ESA method, allows for significantly increasing the efficiency of machines and mechanisms.

Today, the insufficient amount of the data as for the analysis of the PD processes referred to the nanostructured surface layers formed by the

ESA method has been hindering the development of a complex of strengthening technologies. Therefore, it is relevant to carry out the analysis of the surface layer SSS while conducting the surface PD treatment of the ESA layers to determine the algorithm for calculating the technological parameters of the PD processes that provide the necessary strengthening and, accordingly, the operational characteristics of the surface layer and the product itself. The same concerns the experimental studies of the combined ESA+PD processing methods and the development of the technological recommendations referring to the technical problems being investigated.

In our previous studies, we have presented a method for calculating the geometric parameters of the surface layer deformation centres during the ESA processes performed by the hard wear-resistant and soft antifriction materials, when applying the combined electrospark coatings (CECs) having complex structures, as well as, at alloying with a graphite electrode, while the surface layer of the part has been being saturated with carbon, *i.e.*, during the ESC process [93].

It should be noted that, owing to the use of the ESA method, a nanostructure in the coatings can be formed according to several possible mechanisms. They include the crystallisation of the metal from the liquid state thereof and the plastic deformation of the cooled material [95]. In this case, regardless of the electrode materials, a modified layer having a subfine polycrystalline structure appears on the treated surface. By adjusting the processing modes, it is possible to control the dispersion of the crystalline structure of the coating. In addition to the process of grinding, the fine structure blocks and increasing the density of dislocations thereof owing to the use of the ESA method, nanostructuring the coatings can occur due to the use of the anode materials comprising nanocomponents.

In Ref. [96], when studying the process for nanostructuring the steel 35 grade by the electrode-tools made of the WC-based materials with the addition of the Al_2O_3 nanopowders, in the structures of the cathode (sample) coatings, the ordered aggregation formed of the nanoclusters consisting of the nanoparticles having up to 30 nm in size was found. Here, the authors emphasise that the addition of only 1% of the Al_2O_3 nanopowder to the electrode-tool (anode) that is made of the ВК8(VK8) hard alloy increases the efficiency of the formation of the alloyed layer by three times, and the microhardness of the 35 steel coating — by four times.

To create an alloying electrode-tool containing nanoparticles, the technology of self-propagating high-temperature synthesis (SHS) is often used. However, manufacturing the electrode-tools using this method is technologically complex and expensive. Based on the above, it should be noted that there is an urgent need to study the possibility of obtaining nanostructured coatings by the ESA method that should be more effective and simpler, namely, using special technological media (STSM), which are cre-

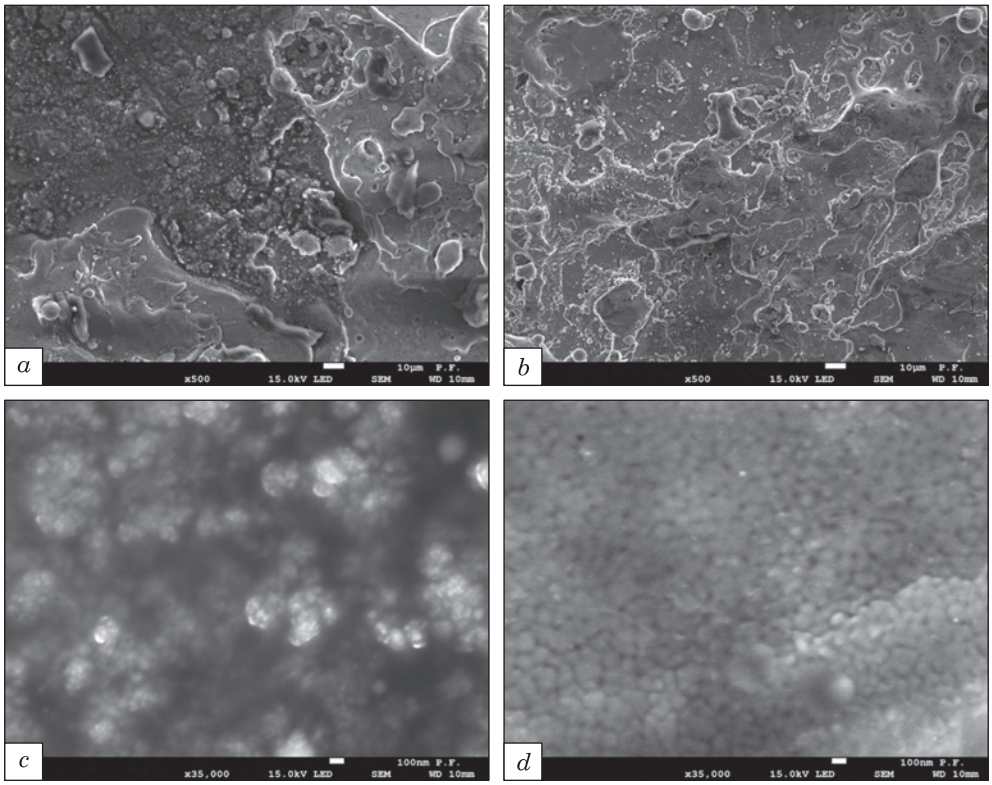

Fig. 11. The alloyed surface appearances of the samples made of Armco iron after the ESA processed by a molybdenum electrode tool and STSM containing ARKEMA carbon nanotubes (0.2 wt.%) in epoxy resin, under different magnifications: (*a, c*) after the ESA of Mo–STSM–Mo at W_p = 0.13 J; (*b, d*) after the ESA of Mo–STSM–Mo at W_p = = 0.52 J [100]

ated between the anode and the cathode (part), and include nanoparticles in a dosed amount.

To form the STSM-containing nanoparticles, there are widely used the special polymers as binders. For the polymeric materials containing nanofillers, the most important issue is the nanofiller dispersion in the polymer volume. In practice, various methods for dispersing the nanofillers in the polymer volume are used [97]. Most often, the nanofillers for the nonmetallic matrix are carbon nanotubes. In [98], it has been established that ultrasonic mixing makes it possible to distribute the nanofillers evenly in the epoxy resin. The use of this method for the nanotube distributions allows avoiding the occurrence of the defects associated with the violation of the structural integrity.

It should be noted that when using the special STSM, the metal surfaces of the parts can be alloyed with both conductive materials and dielectrics [99].

Thus, the development of the technology for increasing the quality parameters of the part surfaces can be achieved by developing a general approach to the conception of combining the technologies for structuring the coatings, which are obtained by ESA processing the metal surfaces with the use of the STSMs comprising the nanotubes, and the PD process, and which approach should be based on the analysis of the SSS of the surface layer.

In Ref. [100], the authors of this paper conducted studies of the samples made of Armco iron, on which molybdenum ET coatings had been ap-

Table 5. **The parameters of the coatings on Armco iron after the ESA process [100]**

Electrode materials, ESA technology	STSM composition	W_p, J	'White' layer thickness, μm	'White' layer microhardness, *HV*	'White' layer continuity, %	Surface roughness R_a, μm
Cathode—Armco iron, anode—Mo	Without STSM	0.13	20–30	446	50	0.98
Cathode—Armco iron, anode—Mo (Stage I—ESA Mo, Stage II—STSM application, Stage III—ESA Mo)	Multi-walled carbon nanotubes ARKEMA (0.2%) in Epoxy 510 epoxy resin without hardener	0.13 0.52	30–40 30–40	608 1300	50 70	1.26 2.67
Cathode—Armco iron, anode—Mo (Stage I—ESA Mo, Stage II—STSM application, Stage III—ESA Mo)	Multi-walled carbon nanotubes CABOT (0.25% by weight) + water with surfactant (sulfanol)	0.13 0.52	30–40 30–40	551 534	80 70	1.60 3.33
Cathode—Armco iron, anode—Mo (Stage I—ESA Mo, Stage II—STSM application, Stage III—ESA Mo)	Single-walled carbon nanotubes Tuball Ocsial (0.01% by weight) in Epoxy 510 epoxy resin without hardener	0.13	30–40	1438	80	1.72
	Single-walled carbon nanotubes Tuball Ocsial (0.6% by weight) in polycarbonate	0.13	40–50	949	40	1.85

plied by the ESA method. In this case, different STSM compositions containing nanotubes were used, namely:

• multi-walled carbon nanotubes CABOT (0.25% by weight) + water with a surfactant (sulfanol);

• multi-walled carbon nanotubes ARKEMA (0.2%) in Epoxy 510 epoxy resin without a hardener;

• single-walled carbon nanotubes Tuball Ocsial (0.01% by weight) in Epoxy 510 epoxy resin without a hardener;

• single-walled carbon nanotubes Tuball Ocsial (0.6% by weight) in polycarbonate.

The samples made of Armco iron were processed in three stages: at the first stage, the surface was alloyed with the ET molybdenum at $W_p = 0.13$ or 0.52 J. At the second stage, the STSM-containing nanoparticles were applied to the surface without waiting for drying thereof, and at

Table 6. **Summarized data of the parameters for the obtained coatings on the samples made of 40X (40Kh) steel, 12X18N10T(12Kh18N10T) steel and high-strength cast iron ВЧ 60 (VCh60) [101]**

Electrode materials, ESA technology	STSM composition	W_p, J	'White' layer thickness, μm	Hardness of the transition layer *HV*, MPa
Cathode—40X (40Kh) steel, anode—Mo	Without STSM	0.13	20–30	663
Cathode—steel 12X18H10T (12Kh18N10T), anode—Mo	Without STSM	0.13	20–30	715
Cathode—ВЧ60 (VCh) cast iron, anode—Mo	Without STSM	0.13	20–30	691
Cathode—steel 12X18H10T (12Kh18N10T), anode–Al	Without STSM	0.52	15–20	245
Cathode—40X (40Kh) steel, anode—Mo (Stage I—ESA Mo, Stage II—application of STSM, Stage III—ESA Mo)	Single-walled carbon nanotubes Tuball Ocsial (0.01% by weight) in Epoxy 510 epoxy resin without hardener	0.13	30–40	1525
Cathode—steel 12X18H10T (12Kh18N10T), anode—Mo (Stage I—ESA Mo, Stage II—application of STSM, Stage III—ESA Mo)			25–40	1632
Cathode—ВЧ60 (VCh) cast iron, anode—Mo (Stage I—ESA Mo, Stage II—application of STSM, Stage III—ESA Mo)			35–45	1575
Cathode—steel 12X18H10T (12Kh18N10T), anode—Al (Stage I—ESA Al, Stage II—STSM application, Stage III—ESA Al)		0.52	25–40	370

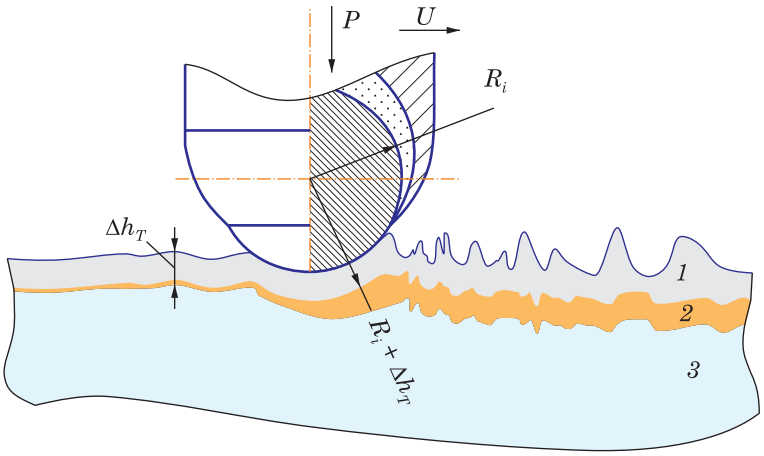

Fig. 12. Diagram of the PD process of the electrospark coatings of the surfaces, using the STSM containing nanotubes: *1* — non-deformable white layer, *2* — strengthened transition layer, *3* — base metal [102]

the third stage, the treatment was repeated by the ESA method with the ET molybdenum at the same discharge energy as at the first stage. For comparison, the samples made of Armco iron without the STSM were studied after alloying them with a molybdenum electrode-tool at $W_p = 0.13$ or 0.52 J.

Due to the analysis of the surface topography of the samples after the ESA process with the ET molybdenum using STSM, it has been found that the formed coatings contain nanosize inclusions that are evenly distributed in the surface layer in Fig. 11.

Introducing the nanotubes to the STSM has a positive effect on the quality indicators of the coatings formed by the ESA method. The greatest effect was obtained when using Tuball Ocsial single-walled carbon nanotubes in the amount of 0.01%. Their introduction to the STSM contributes to an increase in the hardness and continuity of the coating in Table 5.

In [101], in addition to the studies of nanostructuring by the ESA method of the samples made of Armco iron, the study was also conducted on the samples made of 40X (40Kh) steel, 12X18H10T (12Kh18N10T) steel, and high-strength cast iron ВЧ 60 (VCh60) in Table 6.

The previous studies have shown that the microstructures after the ESA process consist of 3 zones: the strengthened upper 'white' layer that is not detected in a reagent, the diffusion zone wherein the hardness gradually decreases to the base, and the substrate having a ferrite structure corresponding to Armco iron.

While ESA processed the samples made of Armco iron by the ET made of molybdenum using the STSM containing the nanotubes, their thickness has been increasing by the thickness of the formed layer (Δh_c). Therefore,

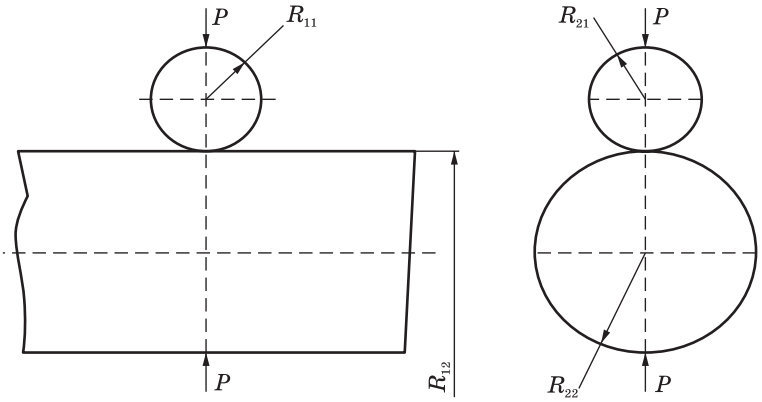

Fig. 13. Scheme of shaft processing by ball rolling and diamond smoothing

if the ESA processes were performed on the surface of the shaft, its diameter would increase by $2\Delta h_c$.

For any material of the electrode-tool (ET), the thickness of the layer formed during the ESA process can be found using the mass transfer equation proposed in Ref. [102], or by measuring it with a micrometre.

Let us consider the change in the geometric parameters of the contacting bodies depending on the structure and microhardness of the surface layers formed during the ESA treatment of the samples made of Armco iron by the ET made of molybdenum with the use of the STSM containing the nanotubes in Fig. 12.

The geometric parameters of the contacting bodies below are corrected, taking into account the parameter of the thickness of the hard 'white' layer ($\Delta h_т$), which is ≈2/3 of the thickness of the applied layer (Δh_c).

At ESA processing Armco iron by the ET made of molybdenum, using the STSM containing the nanotubes, the spherical indenter (Fig. 12), under the influence of the load P applied thereto, indents the hard 'white' layer into a comparatively softer transitional sublayer, with strengthening the latter. The 'white' layer serves as a kind of transmission link by increasing the indenter radius (R_i) by the thickness of the hard 'white' layer ($\Delta h_{wl} = \Delta h_т$) and reducing the diameter of the spherical indenter by $2\Delta h_т$.

According to the contact diagram shown in Fig. 13, it is possible to determine the values of the geometric parameters of the contacting surfaces,

$$\left.\begin{aligned} R_{11} &= R_u, \;\; R_{12} = \infty \\ R_{21} &= R_{11}, \; R_{22} = R_e \end{aligned}\right\}. \qquad (2)$$

Taking into account the parameters of the ESA process for the layer given above, expression (2) will take the form:

$$\left.\begin{aligned} R_{11} &= R_u + \Delta h_{б.с.} = R_u + \frac{2}{3}\Delta h_c;\ R_{12} = \infty; \\ R_{21} &= R_{11};\ R_{22} = R_в + \Delta h_c - \frac{2}{3}\Delta h_c = R_в + \frac{1}{3}\Delta h_c \end{aligned}\right\}. \tag{3}$$

The main curves of the surfaces of the contacting bodies, taking into account the above adjustments, can be determined by the ratio

$$A = \frac{1}{2}\left(\frac{1}{R_u + \frac{2}{3}\Delta h_c} + \frac{1}{\infty}\right);\ B = \frac{1}{2}\left(\frac{1}{R_u + \frac{2}{3}\Delta h_c} + \frac{1}{R_в + \frac{1}{3}\Delta h_c}\right). \tag{4}$$

If $A/B \geq 0.5$, then, the calculation of the given radius of curvature of the contacting surfaces is determined from the ratio

$$D_{pr} = 2R_{pr} = \sqrt{\frac{1}{AB}} = \frac{1}{A}\sqrt{\frac{A}{B}}. \tag{5}$$

Substituting the values of A and B from Eq. (4) and performing the necessary transformations, we obtain:

$$R_{pr} = \left(R_u + \frac{2}{3}\Delta h_c\right)\left(1 + \frac{R_u + \frac{2}{3}\Delta h_c}{R_в + \frac{1}{3}\Delta h_c}\right)^{-1/2}. \tag{6}$$

If $A/B < 0.5$, then,

$$R_{pr} = \frac{\omega}{2A}, \tag{7}$$

where

$$\omega = \frac{2\frac{A}{B}}{n_б n_p\left(1 + \frac{A}{B}\right)}. \tag{8}$$

$n_б$, n_p are the coefficients that depend on the ratio of the principal curves are given in the reference tables.

Considering the values of A and B, we get

$$R_{pr} = \omega\left(R_u + \frac{2}{3}\Delta h_c\right). \tag{9}$$

The residual elimination of the contact centre is determined by the formula:

$$h = \frac{P - P_0}{2\pi \cdot НД \cdot R_{pr}}, \tag{10}$$

where

$$P_0 = P_{0.10}\left(\frac{R_{pr}}{5}\right) = 11\exp[1.9(10^{-3}HД - 1)^{0.668}]\left(\frac{R_{pr}}{5}\right)^2. \qquad (11)$$

Taking into account the above adjustments to the parameters of the contact surfaces, we determine the complete convergence α in the contact and its elastic component α_y. At the beginning, we find the convergence of the bodies in the assumption of purely elastic contact:

$$\alpha_0 = \frac{n_б}{2}\sqrt[3]{\frac{9\pi^2}{4}\left(k_1 + k_2\right)^2 \; p^2 \; \sum K}, \qquad (12)$$

where $n_б$ is a coefficient depending on the ratio of the main curves, and it is determined from the tables; $\sum K = 2(A + B)$ is the sum of the main curves of the surfaces of the bodies at the point of their initial contact,

$$\sum K = \frac{2}{R_u + \frac{2}{3}\Delta h_c} + \frac{1}{R_в + \frac{1}{3}\Delta h_c}, \qquad (13)$$

k_1 and k_2 are elastic constants, and

$$k_1 = \frac{1 - \mu_1^2}{\pi E_1}, \; k_2 = \frac{1 - \mu_2^2}{\pi E_2},$$

μ_1 and μ_2 are Poisson's ratios of the indenter and counter-body materials, E_1 and E_2 are their Young's moduli.

Parameter q can be found from the dependence

$$q = \frac{27}{32}\left(\frac{\alpha_0}{h}\right)^3. \qquad (14)$$

When $q < 1$,

$$\alpha_y = \frac{2h}{3}\left[\cos\frac{1}{3}\arccos\left(2q - 1\right) - 1\right]; \qquad (15)$$

when $q \geq 1$,

$$\alpha_y = \frac{2h}{3}\left[1 + 2\sin^{-1}\left(2\operatorname{arctg}\sqrt[3]{\operatorname{tg}\frac{1}{2}\arcsin\left(\frac{1}{1 - 2q}\right)}\right)\right]. \qquad (16)$$

Therefore, the complete convergence of the bodies in contact is $\alpha = h + \alpha_y$.

To calculate the semi-axes of the residual dent contours a and $в$, we here find the auxiliary semi-axes h_a and h_b:

$$h_a = \frac{2R_{12}h - R_{11}\alpha_y - h^2}{2\left(R_{12} + R_{11} - h\right)} = \frac{2h - \frac{R_{11}\alpha_y}{R_{12}} - \frac{h^2}{R_{12}}}{2\left(1 + \frac{R_{11}}{R_{12}} - \frac{h}{R_{12}}\right)}. \qquad (17)$$

Since $R_{12} = \infty$, then, $h_a = h$,

$$h_b = \frac{2R_{22}h - R_{21}\alpha_y - h^2}{2\left(R_{22} + R_{21} - h\right)}. \tag{18}$$

The semi-axes of the residual dent contours are found using the formulas

$$a = \sqrt{R_{11}\left(2h_a + \alpha_y\right) - h_a^2}, \tag{19}$$

$$в = \sqrt{R_{21}\left(2h_b + \alpha_y\right) - h_b^2}. \tag{20}$$

Then in this case

$$a = \sqrt{\left(R_u + \frac{2}{3}\Delta h_c\right)\left(2h_a + \alpha_y\right) - h_a^2}, \tag{21}$$

$$в = \sqrt{\left(R_u + \frac{2}{3}\Delta h_c\right)\left(2h_в + \alpha_y\right) - h_в^2}. \tag{22}$$

The main macroscopic parameters of the deformation centre during the PD process are the depth of the riveted layer h_s and the intensity of deformation ε_{i0}.

These parameters should be determined by the ratio:

$$h_s = K\sqrt{\frac{P}{2}\left(\frac{1}{\sigma_T} - \frac{1}{НД}\right)}, \tag{23}$$

where

$$K = 1 - \frac{1}{2}\left(1 - \frac{\sqrt{\left(R_u + \frac{2}{3}\Delta h_c\right)\left(2h_b + \alpha_y\right) - h_b^2}}{\sqrt{\left(R_u + \frac{2}{3}\Delta h_c\right)\left(2h_a + \alpha_y\right) - h_a^2}}\right)^4 \tag{24}$$

and

$$\varepsilon_{i0} = 2.4\sqrt[3]{\left(\frac{h}{K^2 R_{pr}}\right)^2\left(\frac{B}{A}\right)^{0.2}}. \tag{25}$$

Thus, the conducted analysis of the stress-stain state (SSS) of the surface layers of Armco iron, steels 40X (40Kh), 12X18H10T (12Kh18N10T), and high-strength cast iron ВЧ 60 (VCh 60) after the ESA process by molybdenum ET using STSM containing nanotubes makes it possible to determine the geometric parameters of the deformation centre and its macroscopic parameters, namely, the depth of the riveted layer h_s and the intensity of deformation ε_{i0}.

11. Conclusions

(i) The studies have shown that due to electric spark carburizing at the expense of the process of concentrated energy flows, an abnormally high diffusion of carbon occurs, and its content in the surface layer can reach 3–4%. Ultra-high-speed hardening, which is implemented by short-term heating to high temperatures with the use of electric discharge, and subsequently instantaneous cooling, leads to the formation of non-equilibrium structures having fine grains, high composition heterogeneity and an increased level of thermal stresses. New environmentally friendly technologies of electrospark carburizing are proposed for practical application.

(ii) It is shown that the use of the ESC process allows to significantly increase the steel part surface layer (up to 72 *HRC*), while the technology is environmentally safe and suitable for the parts made of such sheet steel grades as steel 40X (40Kh), steel 65Г(65G), and 30Х13 (30Kh13) steel, for example, pump blades, screws and disks. The ESC process ensures the formation of non-equilibrium structures, which contribute to increasing the strength and wear resistance of the surface. Ultra-high-speed hardening, which is combined with the process of local plastic deformation, allows controlling the properties of both the surface layer and the base of a sheet material.

(iii) The use of the ESC process before applying hard wear-resistant metals allows for significantly increasing the thickness of the layer of the elevated hardness without deteriorating its mechanical properties. The use of the multilayer combined electric spark coatings (CESC), for example, ВК8 + Cu + ВК8(VK8 + Cu + VK8) in combination with the ESC process provides for a significant increase in the wear resistance of the working surfaces of steel rings for the pulse end seals. Before applying the CESCs, the use of the ESC process allows forming a layer of increased hardness, which in turn improves the adhesion strength between the layers and increases the operational reliability and durability of the parts.

(iv) The ESC process can be effectively used for reducing the hardness of the surface layers of parts, which feature is important for ensuring the tightness and reliability of the stationary component part connections, for example, in the seating positions of steel rings of the pulse end seals. The reduced hardness is regulated by forming a sublayer of the tempering zone or by processing the parts with the use of the ET made of non-ferrous alloys, while the thickness and the mechanical properties of the layers are determined by the discharge energy and the alloying time.

(v) Conducting the ESC process after the ESA treatment with soft antifriction metals effectively reduces the surface roughness and ensures the uniform distribution of the coating material. The use of the intermediate layers of copper or tin bronze contributes to the formation of a reliable metallic bond between the base and the coatings formed of the antifriction

alloys, increasing the durability of such parts as plain bearing liners. Stage by stage application of the layers allows forming the coatings with optimal mechanical properties and roughness, which is important for the operation of tribounits working under high loads.

(vi) The combined electrospark coatings of copper and babbitt on a steel substrate demonstrate high efficiency in forming continuous and uniform surfaces of the parts. The stage-by-stage alloying of copper with accompanying thereof with a decrease in discharge energy allows reducing the roughness and increasing the continuity of the layer, while subsequently applying babbitt ensures providing for the heat accumulation and the uniform spread of drops of the previous layer. This allows achieving a coating thickness of up to 1.0 mm with minimal roughness and high reliability of the metallic bonds between the layers. The optimal thickness of the antifriction layer is 0.25 to 1.0 mm.

(vii) The hybrid technologies based on the ESA method effectively improve the quality of the surface layers of the metal parts. The use of nonabrasive ultrasonic finishing (NAUF) after the ESC process allows reducing R_a to 0.2 to 1.5 μm without losing the thickness of the strengthened layer. To reduce the roughness of the coatings made of soft, antifriction metals applied to the ESC surface of a steel part, it is more expedient to use the ball rolling process, which allows the roughness value to be reduced to R_a = 0.1–0.5 μm, as compared to the NAUF process, where R_a = = 0.80–0.88 μm. They can be used in the friction pairs for running-in the surfaces of the parts or increasing the tightness in the stationary component part connections.

(viii) The stress–strain state of the surface layers after the ESC process and the hybrid technology determines the mechanical properties of the parts, in particular their strength and fatigue resistance. The combination of the ESA method and the surface plastic deformation (PD), such as ball rolling or NAUF, allows optimising the residual stresses, reducing roughness and increasing the microhardness of the layer. Using the concept of the plasticity hardness to calculate the deformation centre allows determining its geometric parameters, as well as macroscopic parameters, namely, the depth of the riveted layer h_s and the intensity of deformation ε_{i0}.

(ix) Modifying the surface layers by the ESA method using a special technological medium (STSM) with carbon nanotubes allows obtaining the nanostructured coatings having an increased wear resistance, solid structure and corrosion resistance. The use of nanotubes in the composition of the STSM contributes to receiving the uniform distribution of the nanocomponents in the coatings, increasing the microhardness and continuity of the layer, and allows controlling the degree of dispersion of the structure. The stress–strain state of the metal surface layers after the ESA method with the subsequent PD process was analysed, and a technique was developed. It allows determining the geometric parameters of the defor-

mation centre and its macroscopic parameters, namely, the depth of the riveted layer h_s and the deformation intensity ε_{i0} in the ESA — nanostructured coatings with evenly distributed carbon nanotubes.

(x) The combined electrospark technologies based on the ESC method allow the formation of strong, wear-resistant and nanostructured surface layers having reduced roughness and high reliability of the metal bonds between the layers. The combination of the advantages of the above technologies ensures the increased durability of the parts.

Acknowledgements. Some of the results have been obtained within the research project 'Development of environmentally safe technologies for surface modification of power plant equipment parts using combined methods based on electrospark alloying' (State reg. no. 0124U000539), Sumy State University, funded by the Ministry of Education and Science of Ukraine.

Authors' Contributions. V.B.T. reviewed and analysed the literature data for Sec. 1 and defined the aim and objectives of the study. Taking into account the possibility of reducing, by electrospark carburizing, the surface roughness of layers formed by the electrospark alloying (ESA) method from soft antifriction metals, the feasibility of applying babbitt coatings to steel surfaces was considered (Sec. 6). The literature data on the stress–strain state of ESC layers, as well as carburised layers with coatings made of soft antifriction materials subjected to surface plastic deformation (SPD), were reviewed and analysed (Sections 7–9). In Sec. 10, O.P.H. analysed the literature data concerning the modification of surface layers of parts by the ESA method using a special technological medium with carbon nanotubes. She supervised the results of this work and wrote the manuscript with the participation of all authors. In Sec. 11, she formulated the general conclusions. N.V.T. and Ie.V.K. collected data on the use of the ESC method to achieve the required properties of surface layers of parts (increase and decrease in hardness, increase in the thickness of the hardened layer, and reduction of its roughness), respectively (Sections 2, 3 and 4, 5). M. A.M. and V.V.P. prepared the tables, figures, and references in accordance with the existing requirements. All authors approved the final version of the manuscript.

REFERENCES

1. V.V. Knysh, S.O. Solovei, B.N. Mordyuk, V.V. Savitsky, O.L. Mikhodui, D.A. Lesyk, and S.I. Motrunich, *International Journal of Fatigue*, **181**: 108147 (2024); https://doi.org/10.1016/j.ijfatigue.2024.108147
2. V.V. Knysh, S.O. Solovei, L.M. Lobanov, O.L. Mikhodui, P.Yu Volosevich, D.A. Lesyk, A.P. Burmak, and B.N. Mordyuk, *Journal of Materials Engineering and Performance*, **33**: 7537 (2024); https://doi.org/10.1007/s11665-024-09355-0
3. L. Nyrkova, V. Knysh, S. Solovei, and S. Osadchuk, *Materials Protection*, **65**: 680 (2024);

https://doi.org/10.62638/ZasMat1052
4. O. Gaponova, C. Kundera, G. Kirik V. Tarelnyk, V. Martsynkovskyy, Ie. Konoplianchenko, M. Dovzhyk, A. Belous, and O. Vasilenko, *Advances in Thin Films, Nanostructured Materials, and Coatings. NAP 2018. Lecture Notes in Mechanical Engineering* (Singapore: Springer: 2019), p. 249; https://doi.org/10.1007/978-981-13-6133-3_25
5. V. Savulyak, O. Shilina, V. Shenfeld, and A. Osadchuk, *Problems of Tribology*, **27**, No. 1/103: 58 (2022).
6. K. Berladir, T. Hovorun, V. Ivanov, D. Vukelic, and I. Pavlenko, *Materials*, **16**: 6877 (2023); https://doi.org/10.3390/ma16216877
7. T. Loskutova, I. Pogrebova, V. Khyzhnyak, I. Smokovich, and N. Nikitina, *Materials Today: Proceedings*, **50**, No. 4: 524 (2022); https://doi.org/10.1016/j.matpr.2021.11.308
8. S. Ben Slima, *Materials Sciences and Applications, Scientific Research Publishing*, **9**, No. 3: 640 (2012); https://doi.org/10.4236/msa.2012.39093
9. O.P. Umanskyi, M.S. Storozhenko, V.B. Tarelnyk, N.V. Tarelnyk, and T.V. Kurinna, *Powder Metallurgy and Metal Ceramics*, **59**, Nos. 1–2: 57 (2020); https://doi.org/10.1007/s11106-020-00138-5
10. V. Subbotina, O. Sobol, V. Belozerov, A. Subbotin, and Y. Smyrnova, *Eastern-European Journal of Enterprise Technologies*, **4**, No. 12 (106): 14 (2020); https://doi.org/10.15587/1729-4061.2020.209722
11. L. Ropyak, I. Schuliar, and O. Bohachenko, *Eastern-European Journal of Enterprise Technologies*, **1**, No. 5: 53 (2016) (in Ukrainian); https://doi.org/10.15587/1729-4061.2016.59850
12. I. Ivasenko, V. Posuvailo, H. Veselivska, and V. Vynar, *International Scientific and Technical Conference on Computer Sciences and Information Technologies*, **2**: 9321900 (2020); https://doi.org/10.1109/CSIT49958.2020.9321900
13. M. Bembenek, M. Makoviichuk, I. Shatskyi, L. Ropyak, I. Pritula, L. Gryn, and V. Belyakovskyi, *Sensors*, **22**, No. 21: 8105 (2022); https://doi.org/10.3390/s22218105
14. M.M. Student, V.M. Dovhunyk V.M., Posuvailo, I.V. Koval'chuk, and V.M. Hvozdets'kyi, *Materials Science*, **53**, No. 3: 359 (2017); https://doi.org/10.1007/s11003-017-0083-x
15. D.B. Hlushkova, V.A. Bagrov, S.V. Demchenko, V.M. Volchuk, O.V. Kalinin, and N.E. Kalinina, *Problems of Atomic Science and Technology*, **4** (140): 125 (2022); https://doi.org/10.46813/2022-140-125
16. O. Poliarus, J. Morgiel, O. Umanskyi, M. Pomorska, P. Bobrowski, M. Szczerba, and O. Kostenko, *Archives of Civil and Mechanical Engineering*, **19** (4): 1095 (2019); https://doi.org/10.1016/j.acme.2019.06.002
17. E. Pakhomova, A. Palombi, and A. Varone, *Crystals*, **15**: 408 (2025); https://doi.org/10.3390/cryst15050408
18. A.K. Thakur, K. Debbarma, A. Pallela, R. Kumar, R. Singh, and S. Srivastava, *Aerospace Systems*, (2025); https://doi.org/10.1007/s42401-025-00418-1
19. X. Meng, W. de Jong, and T. Kudra, *Renewable and Sustainable Energy Reviews*, **55**: 73 (2016); https://doi.org/10.1016/j.rser.2015.10.110
20. T. Mościcki, R. Psiuk, J. Radziejewska, M. Wiśniewska, and D. Garbiec, *Coatings*,

11, No. 11: 1378 (2021);
https://doi.org/10.3390/coatings11111378
21. I.M. Pazukha, A.M. Lohvynov, K.V. Tyschenko, O.V. Pylypenko, Yu.O. Shkurdoda, and V. Komanicky, *MRS Communications*, **14**: 56 (2024);
https://doi.org/10.1557/s43579-023-00499-z
22. I. Pazukha, Y. Shkurdoda, K. Tyschenko, A. Lohvynov, O. Pylypenko, M. Lisnichuk, D. Kondrakhova, V. Latyshev, S. Vorobiov, and V. Komanicky, *Vacuum*, **230**: 113650 (2024);
https://doi.org/10.1016/j.vacuum.2024.113650
23. S. Pylypaka, T. Volina, M. Mukvich, G. Efremova, and O. Kozlova, *Lecture Notes in Mechanical Engineering* (Springer: 2021), p. 63;
https://doi.org/10.1007/978-3-030-50491-5_7
24. S. Pylypaka, T. Zaharova, O. Zalevska, D. Kozlov and O. Podliniaieva, *Lecture Notes in Mechanical Engineering* (Springer: 2020), p. 582;
https://doi.org/10.1007/978-3-030-40724-7_59
25. A.D. Pogrebnjak, A.A. Bagdasaryan, P. Horodek, V. Tarelnyk, V.V. Buranich, H. Amekura, N. Okubo, N. Ishikawa, and V.M. Beresnev, *Materials Letters*, **303**: 130548 (2021);
https://doi.org/10.1016/j.matlet.2021.130548
26. V. Martsinkovsky, V. Yurko, V. Tarelnik, and Yu. Filonenko, *Procedia Engineering*, **39**: 157 (2012);
https://doi.org/10.1016/j.proeng.2012.07.019
27. V.B. Tarelnyk, O.P. Gaponova, E.V. Konoplyantschenko, N.S. Yevtushenko, and V.A. Gerasimenko, *Metallofiz. Noveishie Tekhnol.*, **40**, No. 6: 795 (2018);
https://doi.org/10.15407/mfint.40.06.0795
28. V. Martsinkovsky, V. Yurko, V. Tarelnik, and Yu. Filonenko, *Procedia Engineering*, **39**: 148 (2012);
https://doi.org/10.1016/j.proeng.2012.07.019
29. V. Tarelnyk, I. Konoplianchenko, N. Tarelnyk, and A. Kozachenko, *Materials Science Forum*, **968**: 131 (2019);
https://doi.org/10.4028/www.scientific.net/MSF.968.131
30. O.M. Myslyvchenko, O.P. Gaponova, V.B. Tarelnyk, and M.O. Krapivka, *Powder Metallurgy and Metal Ceramics*, **59**: 201 (2020);
https://doi.org/10.1007/s11106-020-00152-7
31. D.B. Hlushkova, V.A. Bagrov, S.V. Demchenko, V.M. Volchuk, O.V. Kalinin, and N.E. Kalinina, *Problems of Atomic Science and Technology*, **140**, No. 4: 125 (2022).
32. B.A. Liashenko, Ye.K. Solovykh, V.H. Kaplun, N.V. Lypynska, and P.V. Kaplun, *Technological Systems*, **46**, No. 2: 55 (2009) (in Ukrainian).
33. V. Tarelnyk, I. Konoplianchenko, V. Martsynkovskyy, A. Zhukov, and P. Kurp, *Lecture Notes in Mechanical Engineering*, 382 (2019);
https://doi.org/10.1007/978-3-319-93587-4_40
34. Ye.B. Soroka, V.S. Antoniuk, and Ye.K. Solovykh, *Surface Engineering and Product Renovation: Proceedings of the 8th International Scientific and Technical Conference (May 27–29, 2008, Yalta)* (Kyiv: 2008), p. 223 (in Ukrainian).
35. E.K. Solovykh, B.A. Lyashenko, A.V. Rutkovsky, E.B. Soroka, and V.S. Antonyuk, *Technological Systems*, **38**, No. 2: 22 (2007) (in Ukrainian).
36. V.I. Kuzmin, A.A. Mikhal'chenko, O.B. Kovalev, E.V. Kartaev, and N.A. Rudenskaya, *Journal of Thermal Spray Technology*, **21**, No. 1: 159 (2012).
37. A.D. Pogrebnjak, V.I. Ivashchenko, P.L Skrynskyy, O.V. Bondar, P. Konarski, K. Zaleski, S. Jurga, and E. Coy, *Composites Part B-Engineering*, **142**: 85 (2018);
https://doi.org/10.1016/j.compositesb.2018.01.004

38. O. Maksakova, S. Simoēs, A. Pogrebnjak, O. Bondar, Y. Kravchenko, V. Beresnev, and N. Erdybaeva, *Materials Characterization*, **140**: 189 (2018).
39. O.D. Pogrebnjak, K.O. Dyadyura, and O.P. Gaponova, *Metallofiz. Noveishie Tekhnol.*, **37**, No. 7: 899 (2015); https://doi.org/10.15407/mfint.37.07.0899
40. G. Morand, P. Chevallier, L. Bonilla-Gameros, S. Turgeon, M. Cloutier, M. Da Silva Pires, A. Sarkissian, M. Tatoulian, L. Houssiau, and D. Mantovani, *Surface and Interface Analysis*, **53**, No. 7: 658 (2021); https://doi.org/10.1002/sia.6953
41. G. Maistro, S. Kante, L. Nyborg, and Y. Cao, *Surfaces and Interfaces*, **24**: 101093 (2021); https://doi.org/10.1016/j.surfin.2021.101093
42. V.G. Smelov, A.V. Sotov, and S.A. Kosirev, *ARPN Journal of Engineering and Applied Sciences*, **9**, No. 10: 1854 (2014).
43. B. Antoszewski and V. Tarelnik, *Applied Mechanics and Materials*, **630**: 301 (2014); https://doi.org/10.4028/www.scientific.net/AMM.630.301
44. B. Antoszewski, S. Tofil, M. Scendo and W. Tarelnik, *IOP Conf. Ser.: Mater. Sci. Eng.*, **233**: 012036 (2017); https://doi.org/10.1088/1757-899X/233/1/012036
45. V. Tarelnyk, I. Konoplianchenko, O. Gaponova, N. Tarelnyk, V. Martsynkovskyy, B. Sarzhanov, O. Sarzhanov, and B. Antoszewski, *Powder Metall Met Ceram.*, **58**: 703 (2020); https://doi.org/10.1007/s11106-020-00127-8
46. H. Aghajani, E. Hadavand, N.S. Peighambardoust, and S. Khamenehasl, *Surfaces and Interfaces*, **18**, No. 4: 100392 (2020); http://dx.doi.org/10.1016/j.surfin.2019.100392
47. N.E. Kalinina, D.B. Hlushkova, O.D. Hrinchenko, V.T. Kalinin, A.I. Voronkov, L.L. Kostina, I.N. Nikitchenko, T.V. Nosova, and A.A. Reznikov, *Problems of Atomic Science and Technology*, No. 120 (2): 151 (2019).
48. O. Melnyk, O. Onishchenko, S. Kurdiuk, M. Bulgakov, O. Fomin, V. Pнštěk, and P. Kučera, *J. Mar. Sci. Eng.*, **13**, No. 9: 1624 (2025); https://doi.org/10.3390/jmse13091624
49. V.B. Tarelnyk, O.P. Gaponova, V.B. Loboda, E.V. Konoplyanchenko, V.S. Martsinkovskii, Yu.I. Semirnenko, N.V. Tarelnyk, M.A. Mikulina, and B.A. Sarzhanov, *Engin. Appl. Electrochem.*, **57**: 173 (2021); https://doi.org/10.3103/S1068375521020113
50. V.B. Tarelnyk, A.V. Paustovskii, Y.G. Tkachenko, E.V. Konoplianchenko, V.S. Martsynkovskyi, and B. Antoszewski, *Powder Metall. Met. Ceram.*, **55**: 585 (2017); https://doi.org/10.1007/s11106-017-9843-2
51. V. Antonyuk, and L. Lopata, *Problems of Tribology*, **30**, No. 2/116: 77 (2025); https://doi.org/10.31891/2079-1372-2025-116-2-77-83
52. V. Martsynkovskyy, V. Tarelnyk, I. Konoplianchenko, O. Gaponova, and M. Dumanchuk, *Advances in Design, Simulation and Manufacturing II. DSMIE 2019. Lecture Notes in Mechanical Engineering* (Eds. V. Ivanov, Y. Rong, J. Trojanowska, J. Venus, O. Liaposhchenko, J. Zajac, I. Pavlenko, M. Edl, D. Perakovic (Cham: Springer: 2020), p. 216; https://doi.org/10.1007/978-3-030-22365-6_22
53. V.B. Tarel'nik, A.V. Paustovskii, Y.G. Tkachenko, V.S. Martsinkovskii, E.V. Konoplyanchenko, and K. Antoshevskii, *Surface Engineering and Applied Electrochemistry*, **53**, No. 3: 285 (2017); https://doi.org/10.3103/S1068375517030140

54. V.S. Martsynkovskyi, V.B. Tarelnyk, O.H. Pavlov, and A.O. Ishchenko, *Sposib Vidnovlennia Znoshenykh Poverkhon Metalevykh Detalei (Varianty)* [Method for Restoring Worn Surfaces of Metal Parts (Variants)]: *Patent 104664 UA*, IPC B23H 5/00 (Bul. 4) (2014) (in Ukrainian).
55. V.S. Martsynkovskyi, *Sposib Obrobky Vkladyshiv Pidshypnykiv Kovzannia* [Method of Processing Plain Bearing Liners]: *Patent 77906 UA*, IPC B23H1/00, 3/00, 5/00 (Bul. 1) (2007) (in Ukrainian).
56. V.S. Martsynkovskyi, V.B. Tarelnyk, O.H. Pavlov, and A.O. Ishchenko, *Sposib Vidnovlennia Znoshenykh Poverkhon Metalevykh Detalei (Varianty)* [Method for Restoring Worn Surfaces of Metal Parts (Variants)]: *Patent 104664 UA*, IPC B23H5/00, B23H9/00 (Bul. 4) (2012) (in Ukrainian).
57. V.B. Tarel'nyk, O.P. Gaponova, Ye.V. Konoplyanchenko, and M.Ya. Dovzhyk, *Metallofiz. Noveishie Tekhnol.*, **38**, No. 12: 1611 (2016); https://doi.org/10.15407/mfint.38.12.1611
58. V.B. Tarelnyk, O.P. Gaponova, I.V. Konoplianchenko, and M.Ya. Dovzhyk, *Metallofizika i Noveishie Tekhnologii*, **39**, No. 3: 363 (2017); https://doi.org/10.15407/mfint.39.03.0363
59. V.B. Tarelnyk, O.P. Gaponova, I.V. Konoplianchenko, V.A. Herasymenko, and N.S. Evtushenko, *Metallofiz. Noveishie Tekhnol.*, **40**, No. 2: 235 (2018); https://doi.org/10.15407/mfint.40.02.0235
60. V. Tarelnyk, V. Martsynkovskyy, O. Gaponova, N. Tarelnyk, and S. Gorovoy, *IOP Conference Series: Materials Science and Engineering*, **233**, No. 1: 012049 (2017); https://doi.org/10.1088/1757-899X/233/1/012049
61. V.B. Tarelnyk, O.P. Gaponova, N.V. Tarelnyk, and O.M. Myslyvchenko, *Progress in Physics of Metals*, **24**, No. 2: 282 (2023); https://doi.org/10.15407/ufm.24.02.282
62. G.V. Kirik, O.P. Gaponova, V.B. Tarelnyk O.M. Myslyvchenko, and B. Antoszewski, *Powder Metallurgy and Metal Ceramics.*, **56**, Nos. 11–12: 688 (2018); https://doi.org/10.1007/s11106-018-9944-6
63. V. Tarelnyk and V. Martsynkovskyy, *Applied Mechanics and Materials*, **630**: 397 (2014); https://doi.org/10.4028/www.scientific.net/AMM.630.397
64. V. Tarelnyk, V. Martsynkovskyy, O. Gaponova, Ie. Konoplianchenko, A. Belous, V. Gerasimenko and M. Zakharov, *15th International Scientific and Engineering Conference Hermetic Sealing, Vibration Reliability and Ecological Safety of Pump and Compressor Machinery, HERVICON+PUMPS*, **233**, No. 1: 012048 (2017); https://doi.org/10.1088/1757-899X/233/1/012048
65. V.B. Tarelnik, A.V. Paustovskii, Y.G. Tkachenko, V.S. Martsinkovskii, A.V. Belous, E.V. Konoplyanchenko, and O.P. Gaponova, *Surface Engineering and Applied Electrochemistry*, **54**, No. 2: 147–156 (2018); https://doi.org/10.3103/S106837551802014X
66. V. Tarelnyk, O. Gaponova, V. Martsynkovskyy, I. Konoplianchenko, V. Melnyk, V. Vlasovets, M. Mikulina, S. Bondarev, O. Vasilenko, S. Hudkov, A. Kutakh, and G.Golovchenko, *Proceedings of the 2021 IEEE 11th International Conference 'Nanomaterials: Applications and Properties'*, NAP 2021 (2021); https://doi.org/10.1109/NAP51885.2021.9568563
67. B. Antoszewski, O.P. Gaponova, V.B. Tarelnyk, O.M. Myslyvchenko, P. Kurp, T.I. Zhylenko, and I. Konoplianchenko, *Materials*, **14**: 739 (2021); https://doi.org/10.3390/ma14040739
68. O.P. Gaponova, V.B. Tarelnyk, B. Antoszewski, O.M. Myslyvchenko, and J. Hoffman, *Materials*, **15**, No.1: 6085 (2022);

https://doi.org/10.3390/ma15176085
69. A.I. Mikhailyuk, and A.E. Gitlevich, *Surf. Eng. Appl. Electrochem.*, **46**: 424 (2010).
70. Y. Kayali and S. Talaş, *Prot. Met. Phys. Chem. Surf.*, **57**: 106 (2021).
71. O.P. Gaponova and N. V. Tarelnyk, *Metallofiz. Noveishie Tekhnol.*, **44**, No. 9: 1103 (2022);
https://doi.org/10.15407/mfint.44.09.1103
72. V.B. Tarelnyk, O.P. Gaponova, and Ye.V. Konoplianchenko, *Progress in Physics of Metals*, **23**, No. 1: 27 (2022);
https://doi.org/10.15407/ufm.23.01.027
73. T.M. Radchenko, V.A. Tatarenko, H. Zapolsky, and D. Blavette, *Journal of Alloys and Compounds*, **452**, No. 1: 122 (2008);
https://doi.org/10.1016/j.jallcom.2006.12.149
74. V.B. Tarelnyk, V.S. Martsynkovskyi, O.P. Haponova, Ye.V. Konoplianchenko, N.V. Tarelnyk, B.O. Sarzhanov, V.O. Pyrohov, A.D. Lazarenko, and O.O. Hapon, *Sposib Formuvannia Pokryttia na Znoshuvalnykh Poverkhniakh Detalei* [Method of Forming a Coating on the Exposed Surfaces of Parts]: *Patent 141919 UA*, IPC B23H 5/00, B23H 9/00 (Bul. 8) (2020) (in Ukrainian).
75. V.B. Tarelnyk, O.P. Gaponova, and B.O. Sarzhanov, *Ecological Safety and Balanced Use of Resources*, **10**, No. 2 (20): 118 (2019).
76. V.B. Tarelnyk, V.S. Martsynkovskyi, A.V. Bilous, and O.M. Zhukov, *Sposib Pidvyshchennia Znosostiikosti Robochykh Poverkhon Stalevykh Kilets Impulsnykh Tortsevykh Ushchilnen* [Method for Increasing the Wear Resistance of the Working Surfaces of Steel Rings of Impulse Mechanical Seals]: *Patent 114671 UA*, IPC F16J 15/16 (2006.01), F16J 15/34 (2006.01), B23H 9/00, C23C 28/00 (Bul. 13) (2017) (in Ukrainian).
77. V.B. Tarel'nik, V.S. Martsinkovskii, and A.N. Zhukov, *Chemical and Petroleum Engineering*, **53**, Nos. 1–2: 114 (2017);
https://doi.org/10.1007/s10556-017-0305-y
78. V.B. Tarel'nik, V.S. Martsinkovskii, and A.N. Zhukov, *Chemical Petroleum Engineering*, **53**, Nos. 3–4: 266 (2017);
https://doi.org/10.1007/s10556-017-0333-7
79. V.B. Tarel'nik, V.S. Martsinkovskii, and A.N. Zhukov, *Chemical Petroleum Engineering*, **53**, Nos. 5–6: 385 (2017);
https://doi.org/10.1007/s10556-017-0351-5
80. V.B. Tarelnyk, O.P Gaponova, G.V. Kirik, Ye.V. Konoplianchenko, N.V. Tarelnyk, and M.O. Mikulina, *Metallofiz. Noveishie Tekhnol.*, **42**, No. 5: 655 (2020);
https://doi.org/10.15407/mfint.42.05.0655
81. V.S. Martsynkovskyi, and V.B. Tarelnyk, *Sposib Obrobky Spoluchnykh Poverkhon Detalei (Varianty)* [Method of Processing Connecting Surfaces of Parts (Options)] *Patent 66105 UA*, IPC B23H 1/00, B23H 5/00, B23H 9/00 (Bul. 7) (2008) (in Ukrainian).
82. V.S. Martsynkovskyi, V.B. Tarelnyk, Ye.V. Konoplianchenko, and I.O. Oliinyk, *Sposib Obrobky Spoluchnykh Poverkhon Detalei* [Method of Processing Connecting Surfaces of Parts] *Patent 91927 UA*, IPC B23H 1/00, B23H 5/00, B23H 9/00 (Bul. 17) (2010) (in Ukrainian).
83. O.P. Gaponova, V.B. Tarelnyk, V.S. Martsynkovskyy, G.V. Kirik, and A.B. Batalova, *Metallofiz. Noveishie Tekhnol.*, **43**, No. 8: 1121 (2021);
https://doi.org/10.15407/mfint.43.08.1121
84. V.S. Martsynkovskyi and V.B. Tarelnyk, *Sposib Obrobky Vkladyshiv Pidshypnykiv Kovzannia* [Method of Processing Plain Bearing Liners] *Patent 64613 UA*, IPC B23H 1/00, 3/00, 5/00, F16C 33/04 (Bul. 2) (2004) (in Ukrainian).

85. V. Tarelnyk, V. Martsynkovskyy, and A. Dziuba, *Applied Mechanics and Materials*, **630**: 388 (2014);
https://doi.org/10.4028/www.scientific.net/AMM.630.388
86. Ie. Konoplianchenko, V. Tarelnyk, Vs. Martsynkovskyy, O. Gaponova, A. Lazarenko, A. Sarzhanov, M. Mikulina, Zh. Zhengchuan, and V. Pirogov, *Journal of Physics: Conference Series*, **1741**: 012040 (2021);
https://doi.org/10.1088/1742-6596/1741/1/012040
87. V.B. Tarel'nik, V.S. Martsinkovskii, and V.I. Yurko, *Chem. Petrol. Eng.*, **51**: 328 (2015);
https://doi.org/10.1007/s10556-015-0047-7
88. V.B. Tarel'nik, V.S. Martsinkovskii, and V.I. Yurko, *Chem. Petrol. Eng.*, **51**: 402 (2015);
https://doi.org/10.1007/s10556-015-0059-3
89. V.S. Martsynkovskyi, V.B. Tarelnyk, and M.P. Bratushchak, *Sposib Tsementatsii Stalevykh Detalei Elektroeroziinym Lehuvanniam* [Method of Carburizing Steel Parts by Electroerosion Alloying] Patent 101715 UA. IPC, 23H 9/00 (Bul. 8) (2013) (in Ukrainian).
90. V.S. Marcinkovsky, and V.B. Tarelnik, *Method of Strengthening Surfaces of Steel Parts Subjected to Heat Treatment (Variants)* [Method for Strengthening the Surfaces of Heat-Treated Steel Parts (Variants)] Patent 103701, 23H 5/00 (Bul. 21) (2013) (in Ukrainian).
91. V.A. Martsynkovskyi, V.B. Tarelnyk, and B. Antoshevskyi, *Ehnerhoehfektyvni Tekhnolohii Zmitsnennya Metaliv, Alternatyvni Metodam Khimiko-Termichnoi Obrobky* [Energy-Efficient, Alternative and Energy-Saving Technologies] (Sumy: MakDen: 2016), p. 73 (in Ukrainian).
92. V.B. Tarelnyk, V.S. Martsynkovskyi, and M.P. Bratushchak, *Bulletin of Sumy National Agrarian University*, **2**, No. 22: 6 (2010).
93. V.B. Tarelnyk, O.P. Gaponova, Ye.V. Konoplianchenko, V.S. Martsynkovskyy, N.V. Tarelnyk, and O.O. Vasylenko, *Metallofiz. Noveishie Tekhnol.*, **41**, No. 2: 173 (2019);
https://doi.org/10.15407/mfint.41.02.0173
94. A.V. Bilous, *Zabezpechennia Yakosti Robochykh Poverkhon Detalei Vidtsentrovykh Kompresoriv iz Zastosuvanniam Intehrovanykh Tekhnolohii* [Ensuring the Quality of Working Surfaces of Centrifugal Compressor Parts Using Integrated Technologies] (Avtoref. Dysertatsii Kandydata Tekhnichnykh Nauk) (Kharkiv: Natsionalnyi Tekhnichnyi Universytet 'Kharkivskyi Politekhnichnyi Instytut': 2011).
95. D.W. Heard and M. Brochu, *Journal of Materials Processing Technology*, **210**, Nos. 6–7: 892 (2010);
https://doi.org/10.1016/j.jmatprotec.2010.02.001
96. H. Aghajani, E. Hadavand, N.S. Peighambardoust, and S. Khamenehasl, *Surfaces and Interfaces*, **18**, No. 4: 100392 (2020);
https://doi.org/10.1016/j.surfin.2019.100392
97. P.R. Thakre, Y. Bisrat, and D.C. Lagoudas, *Journal of Applied Polymer Science*, **116**, No. 1: 191 (2010);
https://doi.org/10.1002/app.31122
98. A. Yasmin, J.-J. Luo, and I.M. Daniel, *Composites Science and Technology*, **66**: 1179 (2006);
https://doi.org/10.1016/j.compscitech.2005.10.014
99. O.P. Gaponova, B. Antoszewski, V.B. Tarelnyk, O.M. Myslyvchenko, and N.V. Tarelnyk, *Materials*, **14**, No. 21: 6332 (2021);
https://doi.org/10.3390/ma14216332

100. O.P. Gaponova, V.B. Tarelnyk, N.V. Tarelnyk, and O.M. Myslyvchenko, *JOM*, **75**, No. 9 (2023);
https://doi.org/10.1007/s11837-023-05940-1
101. O.P. Haponova, V.B. Tarelnyk, N.V. Tarelnyk, Petro Furmanchyk, V.O. Okhrimenko, and A.V. Tkachenko, *Sposib Modyfikatsii Poverkhnevykh Shariv Detalei Mashyn Metodom Elektroiskrovoho Lehuvannia (EIL) Metalevym Elektrodom Instrumentom u Spetsialnomu Tekhnolohichnomu Seredovyshchi (STNS) z Rivnomirno Rozpodilenymy Vuhletsevymy Nanotrubkamy* [Method of Modifying Surface Layers of Machine Parts by Electrospark Doping (ESD) with a Metal Electrode Tool in a Special Technological Environment (STNE) with Uniformly Distributed Carbon Nanotubes.] *Patent 155786 UA*, IPC B23H 1/00 B23H 9/00 B82B 1/00 (Bul. 15) (2024) (in Ukrainian).
102. V.B. Tarelnyk, O.P. Gaponova, Ye.V. Konoplianchenko, V.S. Martsynkovskyy, N.V. Tarelnyk, and O.O. Vasylenko, *Metallofiz. Noveishie Tekhnol.*, **41**, No. 3: 313 (2019);
https://doi.org/10.15407/mfint.41.03.0313

Received / Final version
02.01.2026 / 03.06.2026

В.Б. Тарельник[1], *О.П. Гапонова*[2,3], *Н.В. Тарельник*[1],
Є.В. Коноплянченко[1], *М.О. Мікуліна*[1], *В.В. Постолатій*[1]
[1] Сумський національний аграрний університет,
вул. Герасима Кондратьєва, 160, 40021 Суми, Україна
[2] Сумський державний університет,
вул. Харківська, 116, 40007 Суми, Україна
[3] Інститут фундаментальних технологічних досліджень
Польської академії наук, 5Б Павіньскєґо, 02-016 Варшава, Польща

ПІДВИЩЕННЯ ПАРАМЕТРІВ ЯКОСТІ СТАЛЕВИХ ПОВЕРХОНЬ КОМБІНОВАНИМИ ТЕХНОЛОГІЯМИ ЕЛЕКТРОІСКРОВОЇ ЦЕМЕНТАЦІЇ. Ч. 1. Властивості металевих поверхонь

Актуальність цього дослідження зумовлено зростанням вимог до забезпечення надійності та довговічності деталей машин, що працюють в умовах інтенсивних механічних навантажень, підвищених температур і дії корозійних середовищ. Сучасні енергоефективні й екологічно безпечні технології поверхневого зміцнення, зокрема електроіскрове легування (ЕІЛ), відкривають широкі можливості для цілеспрямованого модифікування структури та властивостей поверхневих шарів без зміни геометричних параметрів виробів. Метою роботи є аналіз комбінованих електроіскрових технологій формування функціональних покриттів, а також обґрунтування способів удосконалення методу ЕІЛ шляхом використання вуглецевмісних паст (спеціальних технологічних середовищ — СТС) і наноструктурування поверхневих шарів шляхом введення до їхнього складу вуглецевих нанотрубок. Досліджено структурно-фазовий склад та експлуатаційні властивості покриттів, одержаних удосконаленими технологіями ЕІЛ. Розглянуто методи електроіскрової цементації, ЕІЛ твердими зносостійкими та м'якими антифрикційними металами, формування комбінованих багатошарових покриттів, а також гібридні технології, що поєднують ЕІЛ з подальшою поверхневою пластичною деформацією (ППД). Проведено мікроструктурні, трибологічні та механічні дослідження, а також аналіз напружено-деформованого стану поверхневих шарів. Показано, що електроіскрова цементація забезпечує аномально високу дифузію Карбону та формування нерівноважних

дрібнозернистих структур із твердістю до 72 *HRC*. Комбінування ЕІЛ з графітовим електродом з подальшою ППД дає змогу зменшити шорсткість поверхні до R_a = = 0,1–1,5 мкм, підвищити зносостійкість і адгезійну міцність покриттів, а також керувати рівнем залишкових напружень. Використання СТС із вуглецевими нанотрубками сприяє формуванню наноструктурованих покриттів з підвищеною мікротвердістю та корозійною стійкістю. Практичне застосування одержаних результатів полягає у впровадженні комбінованих електроіскрових технологій для зміцнення та відновлення деталей машин, зокрема елементів насосів, ущільнень і підшипникових вузлів, що забезпечує підвищення їхньої надійності та довговічності.

Ключові слова: електроіскрове легування, електроіскрова цементація, комбіновані покриття, мікроструктура, довговічність деталей машин.